


 Cite this: *Sens. Diagn.*, 2022, 1, 1098

## Recent advances in optical sensors for continuous glucose monitoring

 Israr Ahmed,<sup>a</sup> Nan Jiang,<sup>id</sup>\*<sup>b</sup> Xinge Shao,<sup>c</sup> Mohamed Elsherif,<sup>a</sup> Fahad Alam,<sup>a</sup> Ahmed Salih,<sup>a</sup> Haider Butt<sup>a</sup> and Ali K. Yetisen <sup>id</sup><sup>c</sup>

Diabetes has recently become the leading cause of death worldwide. So far, there is no effective treatment to cure or prevent diabetes. Still, reasonable blood control through glucose monitoring can improve treatment efficiency, relieve symptoms, and reduce the complications of the disease. However, conventional glucose detection is based on the finger-prick measurement, which may bring discomfort and pain to patients. Electrochemical-based continuous glucose monitoring (CGM) devices have been commercialized and appreciated by patients. However, those sensors still have high costs, short lifetime, and frequent calibration *via* finger-prick measurement. In recent studies, as a promising method for glucose quantification, optical glucose sensing technology has been considered a potential alternative to electrochemical CGM sensors. A commercial CGM sensor based on fluorescence sensing has been developed and can be worn for a longer period before a replacement. This paper aims to review optical methods for CGM, including near-infrared (NIR) spectroscopy, mid-infrared (MIR) spectroscopy, Raman spectroscopy, photoacoustic (PA) spectroscopy, fluorescence technology, optical coherence tomography (OCT), holographic technology, and hydrogel sensing technology in aspects of principles, current research, and limitations. Discussions and comparisons in these different optical glucose sensing technologies are also conducted. Moreover, the review discusses the future prospects for optical glucose sensing methods and concludes that further optical CGM research should focus on the improvement of data processing methods.

 Received 5th October 2021,  
 Accepted 29th July 2022

DOI: 10.1039/d1sd00030f

[rsc.li/sensors](http://rsc.li/sensors)
<sup>a</sup> Department of Mechanical Engineering, Khalifa University, Abu Dhabi 127788, United Arab Emirates

<sup>b</sup> West China School of Basic Medical Sciences & Forensic Medicine, Sichuan University, Chengdu 610041, China. E-mail: [jiangnansophia@scu.edu.cn](mailto:jiangnansophia@scu.edu.cn)
<sup>c</sup> Department of Chemical Engineering, Imperial College London, London, SW7 2AZ, UK

## 1. Introduction

### 1.1 Clinical significance of diabetes mellitus

Diabetes mellitus (DM) is a metabolic disease characterized by high BGL and seems to have a global epidemic trend in


**Israr Ahmed**

*Israr Ahmed completed his M.Sc. in Physics at Heidelberg University, Germany, in 2017. Currently, he is pursuing his Ph. D. in Material Science & Engineering at Khalifa University, United Arab Emirates. His current research focuses on development of hydrogel-based fiber-optic probes for sensing applications.*


**Nan Jiang**

*Dr. Nan Jiang earned her Ph.D. degree from Wuhan University of Technology. After her PhD study, she worked as a postdoctoral fellow and research associate at Harvard University and Imperial College London. She is currently working as the Principal Investigator in the West China School of Basic Medical Sciences & Forensic Medicine at Sichuan University. Her research is aimed at optical biosensors and microfluidic devices. She has published more than 30 peer-reviewed papers as the first and corresponding author. Some important works have been published in leading journals and selected as “Hot Paper”, “Highly-cited Paper”, and “Cover paper”.*



recent decades. According to the World Health Organization (WHO),<sup>1</sup> between 1980 and 2014, the number of people affected by DM has quadrupled, rising from 108 million to 463 million globally. Some reports predicted that this number would continue to expand. Until 2030, the worldwide diabetic patients' group is estimated to be 578 million with a prevalence rate of 10.2%.<sup>2</sup> Moreover, the number of people who die from diabetes is also climbing annually. From the statistics of the WHO and the International Diabetes Federation, the number of deaths caused by diabetes reached 1.6 million in 2020 and 6.7 million in 2021, for which diabetes was ranked as one of the top 10 causes of death globally.<sup>3,4</sup> This means at the moment, diabetes is consuming one life every 5 s. The diabetes market is gradually expanding with the spread of diabetes worldwide. The sales of the global diabetes market approached \$28.1 billion in 2012 (ref. 5) and reached 57 billion in 2018.<sup>6</sup> It is forecasted that the entire

market for the primary antidiabetic drug: insulin will grow steadily at an average annual rate of about 10%.<sup>7</sup>

## 1.2 Pathophysiology of diabetes

Diabetes is a syndrome due to metabolic disorders caused by insufficient insulin secretion or inappropriate use of insulin. As a common hormone, insulin plays a vital role in maintaining blood glucose concentration *via* stimulating glucose transport into muscle and fat cells while reducing the production of glucose in the liver through gluconeogenesis and glycogenolysis.<sup>8</sup>

Type 1 diabetes (T1D), type 2 diabetes (T2D), and gestational diabetes are the three main types of DM. Among which, type 1 diabetes (T1D) and type 2 diabetes (T2D) have the most significant number of patients, accounting for approximately 99.8% of the total number of patients.<sup>9</sup> T1D,



**Xinge Shao**

*products development.*

*Xinge Shao completed her BSc in Chemistry at the University of Liverpool in 2019 and worked on silver nanoparticle sensors. In 2020, she finished her master's degree in Advanced Chemical Engineering at Imperial College London. During that period, her research focused on optical sensors for glucose monitoring, especially in wearable holographic sensors. She is currently working in BASF as an Engineer on polyurethane*



**Mohamed Elsherif**

*Dr. Mohamed Elsherif completed his Ph.D. in Optical Biosensors at University of Birmingham, UK, in 2019. Currently, he is a postdoctoral research fellow in the Department of Mechanical Engineering, Khalifa University, United Arab Emirates. He is interested in developing fiber-optic probes and wearable sensors that can be used at point-of-care settings.*



**Fahad Alam**

*University of Science and Technology, Saudi Arabia. He is working on 3D/4D printing of polymer composites for biomedical/sensing applications and currently focused on 4D printing of liquid crystal elastomers (LCEs).*

*Dr. Fahad Alam completed his M. Tech in Nanotechnology at Aligarh Muslim University, Aligarh, India in 2012, and Ph.D. in Materials Science and Engineering at Indian Institute of Technology, Kanpur, India, in 2017. He worked as postdoc in Khalifa University with Prof. Haider Butt, in the Department of Mechanical Engineering from April 2018 to March 2022. Currently, he is working as postdoc in King Abdullah*



**Ahmed E. Salih**

*Ahmed E. Salih received his B.Sc. in Mechanical Engineering (High Honors) from the American University in Sharjah in 2018 and M.Sc. in Mechanical Engineering (Highest Honors) from Khalifa University in 2020. Ahmed's main area of interest is the development of hydrogel biosensors and smart contact lenses. He recently developed nanocomposite contact lenses for color-blindness management.*



also called insulin-dependent diabetes, occurs most frequently in children and adolescents. It is attributed to the selective destruction of islet beta cells (B cells), which are the major cells for insulin-secretion<sup>10</sup> and are mainly caused by autoimmune processes depending on factors on both genetic and environmental levels.<sup>11</sup> On the other hand, T2D, also called non-insulin-dependent diabetes, is more common in adults and accounts for around 90% of all diabetes cases. T2D has resulted from insulin resistance with insufficient compensatory insulin secretion, which is likely associated with the development of islet amyloidosis.<sup>9</sup> In contrast to T1D, B cells always exist in T2D but show a lack of functional activities. The phenomenon of the secretory defect of B cells is pronounced in people with obesity, hyperinsulinemia, and insulin resistance.<sup>11</sup> Therefore, these T2D patients are suggested to take drugs or insulin orally to keep their blood glucose under control.

Diabetes itself is not fatal, while complications caused by hyperglycemia and hypoglycemia are often severe illnesses and could lead to death. It commonly includes diseases in the nervous system, blood vessels, and eyes,<sup>12,13</sup> such as glaucoma, cataracts, and cardiovascular disease. According to the American Diabetes Association (ADA), about half of diabetes patients have some degree of nerve damage. In addition, people with diabetes require more attention to their cardiovascular health. In the study from Sandesara's group,<sup>14</sup> among 1109 subjects, about 32% of diabetic patients had at least one microvascular complication, and they were at a higher risk of hospitalization due to heart failure.

Besides diabetes, pre-diabetes is also getting a lot of attention because it can lead to T2D and heart problems in normal people. Prediabetes is a state of intermediate hyperglycemia. In other words, a person is considered pre-diabetic when the glucose level in his blood is higher than the normal value but still less than the diabetic condition. Impaired fasting glucose (IFG) and impaired glucose tolerance (IGT) are identified as pre-diabetic conditions.<sup>15</sup> IFG is identified as having abnormal fasting plasma along with 2 hour post-challenge plasma glucose in the order of  $<7.8 \text{ mmol l}^{-1}$ . On the other hand, IGT is described as having a normal fasting glucose level of  $<6.1 \text{ mmol l}^{-1}$  and an abnormal 2 hour post-challenge plasma glucose. Since this topic of pre-diabetes is beyond the scope of this review, just an introduction to IFG and IGT is added here.

### 1.3 Importance of continuous glucose monitoring

In the last few decades, the number of diabetic patients has experienced an astonishing growth, making diabetes a chronic disease that has aroused widespread concern worldwide. Although diabetes is not a fatal disease, it could lead to a series of severe complications and even death.<sup>16</sup> Therefore, it is acknowledged that blood glucose monitoring is essential for diabetes management.<sup>17</sup> The conventional method for glucose quantification is the finger-prick measurement which accesses blood in fingertip capillaries and measures glucose concentration through an enzyme electrochemical reaction. However, frequent pricking measurements can bring



**Ali K. Yetisen**

*Dr. Ali K. Yetisen researches optical biosensors, wearable devices, implantable chips, and personalized medicine. He was previously a Tosteson postdoctoral fellow at Harvard University. He holds a PhD degree in Chemical Engineering and Biotechnology from the University of Cambridge. Dr. Yetisen has been awarded several international prizes including IChemE Nicklin Medal, Birmingham Fellowship, and*

*Alexander von Humboldt Fellowship. He is a Fellow of the Royal Society of Chemistry and the Institute of Physics. Dr. Yetisen has been the driving force for the establishment of several spinout companies.*



**Haider Butt**

*Dr. Haider Butt did his M.Phil. in Electrical Engineering at the University of Cambridge in 2008, followed by a PhD in Nanophotonics in 2012. He was appointed as a Lecturer of Nanotechnology at the Department of Mechanical Engineering, University of Birmingham, UK. He was promoted to Senior Lecturer in 2016 and was appointed as the Senior Admissions Tutor for Mechanical Engineering in 2017.*

*In 2019 he joined Khalifa University, UAE as an Associate Professor. Dr. Butt has published over 150 peer-reviewed articles in prestigious journals and has received research funds of value over 1 million USD. He has earned international recognition for his research in the area of optical sensors, where he has contributions to nanoscale devices by conceiving novel holographic lithography methods to produce optical transducers. His most pioneering works include glucose sensing contact lenses, contact lenses for color blind patients and carbon nanotube based holograms.*



discomfort and pain to patients, leading to an increase of risks of infection and tissue damage.<sup>18</sup> For diabetic patients, it's essential to know and control the blood glucose level, which varies throughout the day. For DM patients, 3–4 times of finger pricking is needed to avoid any complications generated because of hypo and hyperglycemia. Therefore, finger-pricking is not suitable for several measurements a day. This conventional method provides the blood glucose levels for the time they are taken. So, this means that it cannot predict the future blood glucose levels and any fluctuation that happens afterward. For example, these measurements can't be taken during sleep, increasing the risk of high and low blood sugar levels. For diabetic patients, the treatment is vital in case of ups and downs in blood glucose levels. This problem leads to the need for a device with the ability to monitor continuous and real-time glucose levels 24/7.

Continuous glucose monitoring (CGM) is the term used for devices which can monitor the real-time blood glucose level round the clock. Therefore, CGM sensors can measure the dynamic changes in blood glucose levels for DM patients. For example, measuring blood glucose levels during physical activity is of utmost importance. For example, a CGM sensor was employed to monitor DM patients' dynamic blood glucose levels during a marathon.<sup>19</sup> The measurements were recorded for hypo and hyperglycemia during and after the marathon of 42/15 km. A total of 247 readings were recorded for 257 min of running. In addition, a study of dynamic blood glucose changes in DM patients due to cystic fibrosis disease was also reported.<sup>20</sup> Therefore, CGM is vital for diabetic individuals to maintain a healthy and balanced lifestyle by controlling diet, physical activity, and timely medicine intake by knowing real-time blood glucose levels.

Currently, advanced sensors are developed for CGM, which are mainly based on the electrochemical approach. CGM devices measure the concentration of glucose in interstitial fluid (ISF), whose glucose level can be representative of blood glucose level (BGL).<sup>21</sup> Companies include Medtronic, Abbott, and Dexcom, which have contributed to the development of CGM devices and have successfully commercialized several generations of CGM sensors, leading the market of wearable CGM sensors. Also, CGM sensors have potential in subcutaneous tissue glucose monitoring as some of the CGM sensors are implanted in subcutaneous tissues. For example, most CGM sensors are implanted under the skin to record blood glucose levels. Many studies have reported blood glucose monitoring in subcutaneous tissues.<sup>22</sup> But there are limitations for the implanted sensors like size, shape, duration of implantation and biocompatibility of the sensor with human tissue.

Nevertheless, those electrochemical-based glucose sensors still have issues in terms of long lifetime, portability, and accuracy.<sup>17</sup> Therefore, researchers tried to find and develop alternatives to these sensors and create more affordable, invasive/minimally invasive, and user-friendly CGM sensors.<sup>23</sup> Optical measurement is a promising platform for glucose sensing. Some technologies have been reported with high

potential in continuous glucose sensing, including spectroscopy (NIR, MIR, Raman), fluorescence, holographic technology, *etc.*<sup>17,23</sup> It is noticeable that a CGM sensor based on fluorescence sensing, called Eversense, has been developed by Senseonics Company and put on the market. This fluorescence-based sensor presents a much longer lifespan in comparison with electrochemical sensors.<sup>24</sup>

This review mainly focuses on optical technologies in CGM since they have advantages in reagent-free measurements and a longer lifespan. Seven optical methods will be introduced in terms of measuring principles, research statutes, and current challenges. Studies in both invasive and non-invasive measurements will be presented. In addition, the mainstream CGM devices on the market will be introduced and compared with these optical technologies. A discussion of optical measurement approaches and a future outlook for these technologies are also included.

## 2. Existing glucose monitoring approaches

### 2.1 Self-monitoring of blood glucose–SMBG

SMBG devices, also termed non-continuous monitoring devices, are glucometers developed for diabetic patients who require constant monitoring of their blood sugar levels. The device assesses the capillary blood glucose by finger pricking with a lancet, and the reaction mechanism is enzyme-electrochemical based (Fig. 1A). As shown in Fig. 1B, the whole process will proceed on a glucose test strip which will transfer electrons to a meter.<sup>16</sup> Three electrodes are included in a test strip, including a working electrode sensing the amount of current, a reference electrode keeping the voltage at a constant level, and a counter electrode offering the current to the working electrode. When a drop of the blood sample is placed on the center of the working electrode, the coated enzyme will oxidize the glucose. As a result, a certain amount of current will generate, proportional to the glucose concentration. Then the electrons travel to the meter containing a current-to-voltage converter that can produce a voltage proportional to the glucose level. Finger-prick measurement is the most prevalent method for people with diabetes to check whether the BGL is within healthy physiological boundaries.<sup>25</sup> Therefore, it is recommended that T1D patients monitor their BGL, which requires at least 3–4 times finger-pricking measurements per day.<sup>26,27</sup>

However, finger-pricking has several disadvantages. The continuous blood sampling process is inconvenient, potentially expensive, and brings patients significant pain and long-term problems for sensitive fingers.<sup>26</sup> In addition, finger-pricking may carry a risk of infection and damage fingers in the long term.<sup>18</sup> Aside from pain, this measurement only provides blood glucose data obtained at a single point of time which does not accurately reflect the true BGL of the patient.<sup>17,30</sup> Thus, a finger-prick glucose measurement device is not practical for continuous glucose monitoring. Some occurrences of hyperglycemia or



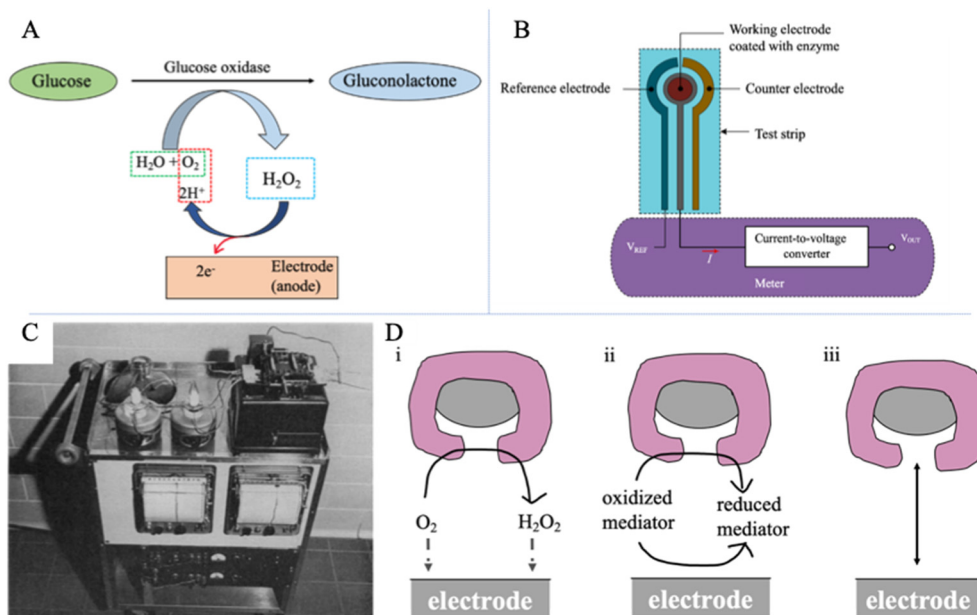


**Fig. 1** Electrochemical glucose sensing. (A) Mechanisms of the enzyme-catalyzed glucose oxidation. Glucose is oxidized by oxygen with an enzyme (glucose oxidase) and produces current via hydrogen peroxide dissociation. (B) The schematic diagram of a SMBG device via finger-prick measurement.<sup>16</sup>  $V_{REF}$  is the reference electrode's voltage,  $V_{OUT}$  is the converted voltage proportional to the glucose value, and  $I$  is the current. Reproduced from ref. 16 with permission from MPDI, Copyrights 2019. (C) Blood gas analyzer with the two-channel unit for glucose measurement.<sup>28</sup> Reproduced from ref. 28 with permission from Scientific Research Publishing Inc, Copyrights 1962. (D) Three generations of amperometric enzyme electrodes for glucose based on the use of (i) a natural oxygen cofactor, (ii) artificial redox mediators, and (iii) direct electron transfer between glucose oxidase and the electrode.<sup>29</sup> Reproduced from ref. 29 with permission from ACS, Copyrights 2008.

hypoglycemia may not be recorded between two measurements which can bring risks to diabetic patients.<sup>18</sup>

## 2.2 Commercial continuous glucose monitoring (CGM) devices

As the finger-prick glucometer cannot ideally maintain the glucose level stable or predict the occurrence of high or low blood glucose concentration in advance, researchers turned their interest to exploring CGM technology to obtain more detailed information on BGL changes for the diagnosis and treatment of diabetes. Compared with the traditional single-point blood glucose detection, CGM technology provides patients with a real-time concentration of blood glucose and the tendency of blood glucose change, which becomes the best solution for patients to monitor their BGL.<sup>31</sup> In addition, the ideal treatment system for diabetes is to combine CGM detection technology with an automatic insulin delivery system to create a closed-loop control (also known as the artificial pancreas) of blood glucose concentration.<sup>32</sup> This automated system can then release a suitable amount of insulin based on the real-time glucose level and further maintain the stability of the blood glucose concentration. Moreover, real-time CGM has an advantage on significant safety since it will warn users when their glucose level is not in the defined glycaemic threshold,<sup>30</sup> which offers better glycaemic control in adults and children with T1D<sup>33</sup> as well as in insulin-treated patients with T2D.<sup>34</sup>

The broad prospects of a real-time CGM system have aroused attention from many companies, and a series of

products have been developed. Among them, some CGM systems were successfully commercialized and currently become popular among diabetic patients, including MiniMed Guardian 3 (produced by Medtronic), G6 Mobile (produced by Dexcom), FreeStyle Libre (produced by Abbott), and Eversense (produced by Senseonics). A typical CGM system includes a patch with a thin needle that can puncture into the skin and a sensor on the needle providing a real-time blood glucose value. Thus, real-time CGM can offer a long-term measurement for ISF glucose concentration.<sup>35</sup> The sensing system of devices from Medtronic, Dexcom, and Abbott performs based on the enzyme-electrochemical reaction, which uses glucose oxidase (GOx) as the enzyme to oxidize glucose molecules present in the ISF. While as one of the latest CGM technologies, Eversense developed by Senseonics relies on a fluorescence-based sensing system. It is the only commercialized optical glucose sensor in the current market.

As the earliest group of companies exploring commercialized CGM, Medtronic, Dexcom, and Abbott account for the most significant market ratio in CGM devices.<sup>17</sup> The first CGM system, approved by the America Food and Drug Administration (FDA), was the continuous glucose monitoring system (CGMS) from Medtronic MiniMed.<sup>36</sup> Fig. 2A displays the images of Medtronic MiniMed CGMS and its placement on the skin.<sup>37–39</sup> The sensor system consists of four units: a palm-sized glucose monitor, a disposable subcutaneous sensing probe with an external electrical connector, connecting cables, and a data



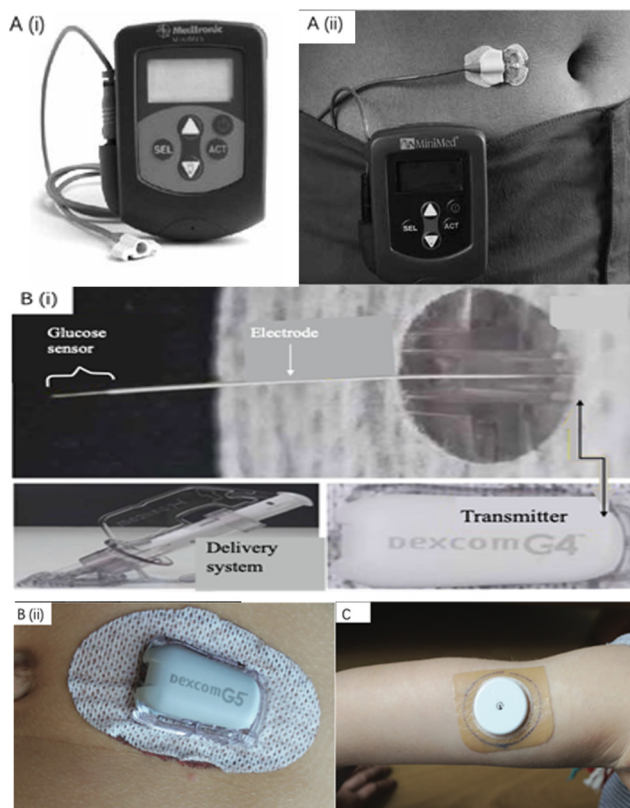


**Fig. 2** Commercialized wearable CGM devices. (A) The Medtronic MiniMed CGMS and its components. A demonstration diagram on how MiniMed CGMS works.<sup>39</sup> Reproduced from ref. 39 with permission from NIHR, Copyrights 2009. (B) CGM systems manufactured by Dexcom company. (i) Components of the Dexcom G4 Platinum sensor for continuous glucose monitoring.<sup>43</sup> The glucose sensor part is inserted under human skin. Reproduced from ref. 43 with permission Springer Nature, Copyrights 2017. (ii) G5 Mobile manufactured by Dexcom is placed on human skin.<sup>42</sup> (C) Abbott FreeStyle Libre is placed on the arm for continuous glucose monitoring.<sup>42</sup> Reproduced from ref. 42 with permission from Wiley, Copyrights 2019.

storage communication device. The first version of Medtronic MiniMed CGMS can offer around 3 days of continuous monitoring of glucose concentration in ISF with a real-time measurement for every 5 minutes and provides a retrospective analysis report for diabetic patients.<sup>36</sup> This CGM system was further developed, and in 2016, Medtronic launched MiniMed Guardian 3 as the latest generation of CGM.<sup>40</sup> The next U.S. market-approved CGM device was created by Dexcom, Inc., (San Diego, CA) in 2006, and the sensor was named DexCom Short-Term Sensor. The sensor system is similar to the MiniMed CGMS. Dexcom has further developed this CGM system and has successively introduced Dexcom G4 Platinum and G5/G6 Mobile in the past decade. They were all approved by the US FDA for the routine treatment of diabetes.<sup>30,34</sup> Fig. 2B shows the images of the components of Dexcom G4 Platinum and how Dexcom G5 Mobile is placed on the skin. It is noticeable that Dexcom's glucose sensors can send real-time glucose readout to smart devices for analysis *via* Bluetooth, eliminating the use of

cables, improving comfort for wearable devices. For the G5 Mobile glucose sensor, twice daily fingerstick tests are required for the calibration of the device,<sup>34</sup> which means that the finger pain caused to patients has not been eliminated. This problem was solved by introducing G6 Mobile, the latest generation of Dexcom CGM sensor. Abbott Diabetes Care (Maidenhead, UK) is the next company that received FDA approval for their CGM system, FreeStyle Navigator, which only requires 4 times finger-prick calibration in 5 days with glucose concentration measurements every minute. This sensor is also based on the same principle as MiniMed CGMS. Abbott further improved the CGM sensor and launched FreeStyle Libre, as the latest generation. FreeStyle Libre totally does not require finger-prick calibrations and can offer measurement up to 8 hours of ISF glucose concentration.<sup>41</sup> As shown in Fig. 2C, the FreeStyle Libre could be applied on the arm to monitor glucose concentration.<sup>42</sup> Furthermore, Abbott FreeStyle Libre can maintain blood glucose dynamic monitoring for up to 14 days which is the longest lifespan of all electrochemical-based glucose sensors.<sup>41</sup>

The Eversense CGM system, a novel device in wearable medical sensors, was developed by Senseonics Company, received the Conformité Européenne (CE) mark in 2016, and entered the European market.<sup>17</sup> Unlike electrochemical-based glucose sensors, Eversense utilizes boronic-acid derivatives as the fluorescent indicator to sense glucose. Similarly, the Eversense CGM System consists of an implantable glucose detecting sensor, a removable transmitter closely connected with the sensor, and a data receiver (smartphone app) that collects signals from the transmitter, as presented in Fig. 3A.<sup>24</sup> The small sensor with a size of  $3.3 \times 15$  mm is coated with a polymer case consisting of an LED for fluorophore excitations and two photodiodes for fluorescent signal measurements. Glucose indicating hydrogel, covering the outside of the sensor, contains the boronic-acid derivative (*i.e.*, the fluorophore), which can reversibly bind with glucose molecules. As shown in Fig. 3B and C, it was proved that the Eversense CGM system could offer an accurate prediction of BGL by comparison between BLG measured by finger-prick glucometers and glucose concentration predicted by Eversense.<sup>24</sup> The sensor has a long lifetime, providing continuous monitoring up to 90 days before replacement. However, it must be subcutaneously inserted *via* a small surgical incision by the physicians, and this may cause a risk of infection and bring discomfort to users. Like many CGM systems, the Eversense also requires finger-prick calibrations with a frequency of twice per day. All mentioned four companies have the most advanced wearable devices for minimally invasive glucose monitoring in the market. They kept their technologies up to date and launched the new generations of their CGM systems. Table 1 concludes several relevant characteristics of those latest sensors, including Medtronic MiniMed Guardian 3, Dexcom G6 Mobile, Abbott FreeStyle Libre, and Senseonics Eversense CGM systems.<sup>17,24,40</sup> By comparison, Senseonics Eversense may be preferred by patients requiring a long-wear and relatively



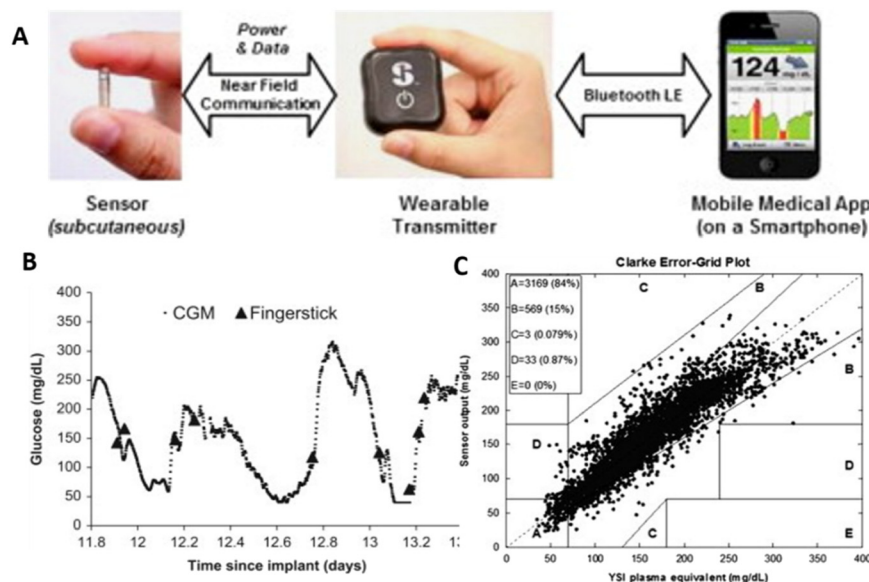


**Fig. 3** The Senseonics Eversense CGM system.<sup>24</sup> (A) Three components of the Eversense CGM system and how they are connected. (B) Clinical results for the Eversense CGM system. Data curve collected by the Eversense CGM system from one subject. Almost all finger-prick measured glucose values correspond to points on the curve. Two hyperglycaemic and two hypoglycaemic episodes were captured by the Eversense CGM system measurements but not by SMCG finger-prick measurement. (C) CGE analysis for all clinical measurements obtained. 99% of measurements were in the combined A and B zones. Reproduced from ref. 24 with permission from Elsevier, Copyrights 2014.

**Table 1** Comparison of four latest commercial CGM systems

Company and product	Medtronic MiniMed Guardian 3	Dexcom G6 Mobile	Abbott FreeStyle Libre	Senseonics Eversense
Organisation approval time	September 2016 (FDA)	March 2018 (FDA)	September 2017 (FDA)	June 2016 (CE)
Accuracy (mean ARD%)	10.55% (abdomen, age 14+)	9% (age 18+)	9.7% (age 18+)	11.1% (age 18+)
Sensor size	9.5 mm long (90 degree insertion)	Not disclosed	5 mm long (90 degree insertion)	15 mm long (90 degree insertion)
Calibration frequency (per day)	Min: 2 (3–4 recommended)	0 (factory calibration)	0 (factory calibration)	2 (every 12 hours)
Sensing molecule	Glucose oxidase	Glucose oxidase	Glucose oxidase	Boronic-acid derivative
Lifetime of sensor (days)	7 (including 2 hours warmup)	10 (including 2 hours warmup)	14 (including 10 hours warmup)	90
Cost	Around \$452 per month (30 days). Including rechargeable transmitter: \$1100 (1 year warranty, may last longer); sensors: \$450 for a box of 5 (35 days' supply)	Min: \$450 per month (30 days). Including transmitter: \$300 (per 90 days); sensors: \$420 (30 days' supply); receiver (not necessary if using smartphone): \$380	Min: around \$144 per month (30 days). Including sensors: \$135 (28 days' supply); reader (not necessary if using smartphone): \$175	Around \$117 per month (30 days). Including sensor + transmitter + supplies + cost of insertion by doctors: \$1400; limited time Eversense Bridge program limits the cost to \$99 plus insertion
Integration with pump	Yes and no: the Guardian 3 is part of the 670 g hybrid closed-loop insulin pump system. The Guardian Connect is a standalone CGM that does not connect to any pump	Tandem t-slim X2 insulin pump with Control-IQ (and older Basal-IQ)	No	No
Data sharing	Up to 4 people with CareLink™ Connect web	Up to 10 people with Dexcom Follow app	Up to 20 people with LibreLinkup app	Up to 5 people with Eversense Now app
Separate receiver available	No	Yes	Yes	No



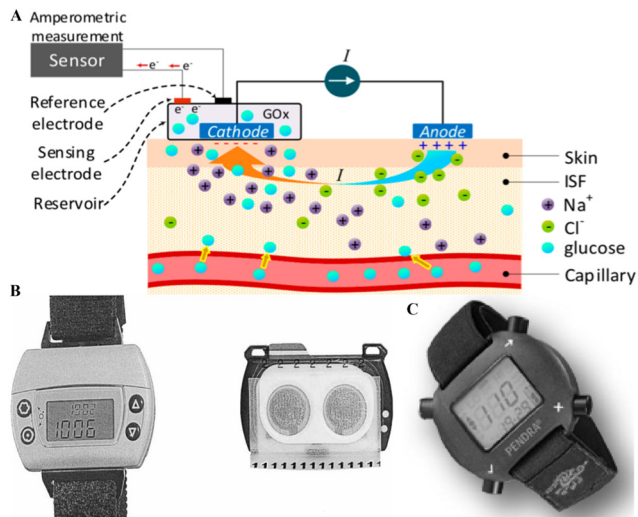


**Fig. 4** Non-invasive CGM systems. (A). The schematic diagram of the principle of glucose monitoring *via* reverse iontophoresis.<sup>16</sup> This technology can access a small amount of ISF *via* the circulation of a small electric current generated by the anode and cathode located on the skin surface. The movement of  $\text{Na}^+$  introduces the current, causing a convective flow (*i.e.*, electrical osmotic flow) in ISF, resulting in glucose molecules in ISF moving towards the cathode. Then, the glucose concentration could be measured by the enzymatic method on the cathode side. For example, oxidation could happen in a sensor containing GOx. Reproduced from ref. 16 with permission from MPDI, Copyrights 2019. (B) The photograph of the GlucoWatch CGM system. It includes a sensing pad (called GlucoPad) and a watch-style monitor. The GlucoPad is placed on the back of the watch during working and is disposable and detachable.<sup>47</sup> Reproduced from ref. 47 with permission from Wiley, Copyrights 2002. (C) The photograph of the Pendra glucose sensor.<sup>48</sup> The Pendra CGM system includes a watch-style case for display signals for glucose concentrations. Reproduced from ref. 48 with permission from Hindawi, Copyrights 2011.

affordable system (approximately \$117 per month). For those with high accuracy requirements, the Dexcom G6 Mobile may be a better choice.

Aside from these four market-dominating devices, some companies were in the exploration of non-invasive CGM sensors. The two typical examples are GlucoWatch (Cygnus Inc.) and Pendra (Pendragon Medical Ltd.). GlucoWatch, as a well-known non-invasive technology, measures the concentration of glucose based on the reverse iontophoresis process (Fig. 4A), which uses an electric current to extract glucose molecules out of the body tissues across the skin.<sup>44</sup> This technology was developed by the University of California (San Francisco) and Cygnus Therapeutic Corporation (Redwood City, CA) and was approved by the FDA.<sup>44</sup> Fig. 4B presents the photograph of the GlucoWatch CGM system. This device includes a sensing pad that can easily adhere to human skin, called GlucoPad, and it could offer measurement and readouts of glucose concentration electrochemically. However, daily replacement is needed for the GlucoPad with calibration by finger-prick measurement. Although the GlucoWatch is the only device broadly described as ‘non-invasive’, it did not survive for a long time in the market at the end since the GlucoWatch did not show expected reliability and consistency.

Moreover, the current generated by the device could result in severe skin irritation, such as reddening, burning, and even blisters.<sup>44</sup> Another CGM system is Pendra, initially introduced by Pendragon Medical and approved by CE in 2003.<sup>45</sup> As shown in Fig. 4B, Pendra resembles a digital wristwatch and can offer continuous monitoring without pain and trauma. The glucose value is provided based on the indirect measuring process termed impedance spectroscopy which is related to the transportation of sodium ions over the erythrocyte membrane to indicate the change of the glucose level.<sup>45</sup> When the sensor plate touches the skin, it will generate a small electromagnetic field with 1–2 MHz frequency.<sup>46</sup> Under this particular resonance frequency, the sensor's impedance is defined by the impedance changes of the skin and inner tissues. With the changes in the glucose level, the conductivity of the tissue membrane changes slightly due to the fluctuation in sodium ( $\text{Na}^+$ ) and potassium ( $\text{K}^+$ ) ions, and the sensor device can detect this by the changes in impedance.<sup>46</sup> However, Pendra has a similar fate to GlucoWatch. It only appears in the market for a short time. Some studies pointed out that the correlation between the Pendra obtained glucose value and the self-monitoring obtained blood glucose value was only 35.1%.<sup>45</sup> Due to the poor accuracy, the Pendra glucose sensor was reported as an unsuitable device for a large group of patients according to the skin and underlying tissue.<sup>45</sup> Overall, there is no currently commercialized non-invasive CGM system in the wearable sensor market, and research is still needed in this area.

Although current commercial CGM devices provide a relatively convenient and minimally invasive measurement for real-time continuous glucose concentration monitoring of diabetes patients, the bulk volume of the device and the implantation of the sensor probe still bring discomfort to the patients.<sup>35</sup> Furthermore, the cost of CGM systems is relatively high, which means that not all patients can afford those devices in their daily life.<sup>49</sup> Therefore, researchers are actively looking for minorly invasive or non-invasive and more economical ways to diagnose diabetes.

### 3. Current sensing technologies

#### 3.1 Electrochemical glucose sensing

Electrochemical glucose biosensors have received greater attention and developed well in the past decade. Electrochemical techniques perform well in terms of high accuracy and reaction specificity. Moreover, they are preferable in point-of-care and home monitoring (*i.e.*, SMBG and CGM) due to their simplicity and relative affordability.<sup>16</sup> Currently, the mainstream, wearable glucose sensors on the market are all enzyme-electrochemical based.

The electrochemical glucose sensing is based on the enzyme-catalyzed glucose oxidation reaction. Fig. 1A presents the mechanism of the process. GOx is an enzyme that is specific to glucose. Thus, in this method, glucose was oxidized by oxygen ( $\text{O}_2$ ) in the presence of GOx and water ( $\text{H}_2\text{O}$ ) to form gluconolactone and hydrogen peroxide ( $\text{H}_2\text{O}_2$ ). Hydrogen peroxide is further oxidized at the electrode



(anode), producing free electrons, resulting in an electrical current proportional to the glucose concentration in the immediate area.

The first enzyme-based electrochemical glucose sensor was developed in 1962 by Clark and Lyons<sup>28</sup> and launched by YSI (Yellow Springs Instruments) company in 1975 (Fig. 1C). The first commercial blood glucose analyzer (YSI Glucose Analyzer) directly quantifies the glucose concentration and allows a small amount of blood sample analysis. They designed and developed the glucose oxidase-coated electrode by using a semi-permeable membrane to immobilize oxidase on the surface of the oxygen electrode.<sup>28</sup> Glucose diffuses through the semi-permeable membrane and reacts with GOx. When the hydrogen peroxide is oxidized, the oxygen consumption rate near the surface of the oxygen electrode is measured. Then, the glucose concentration in the sample can be determined by the proportional decreasing rate of oxygen consumption and the loss of electrons. With the development of electrochemical glucose sensing, new generations of electrochemical glucose sensors appeared. Wang divided these electrochemical glucose sensors into three development stages according to different electron transfer mechanisms, as shown in Fig. 1D.<sup>29</sup> He concluded that the process is *via* natural substrates, artificial redox mediators, or direct electron transfer and pointed out that the transportation of charges between the redox center and electrodes requires further improvements. With more profound research of the electrode design, enzyme immobilization method, and polymer film, researchers have successively developed novel enzyme electrode glucose detection equipment. This electrode has higher sensitivity and anti-interference ability, which has promoted electrochemical glucose sensor development.

The inhibition of the enzyme and electron transfer in enzyme-based electrochemical sensors results in interference problems. Many non-enzyme electrochemical sensors have been reported in recent years to overcome this problem. The enzyme-based catalysts can be replaced with an alternative catalyst such as functionalized nanomaterials, metal-oxides, and composites.<sup>50–54</sup> The sensing capability of these sensors is mainly controlled by material composition and morphology. The sensitivity of these sensors depends upon the electrode's surface area, which allows direct glucose oxidation. The surface modification of electrodes can be done using active nanomaterials, which serve as electrocatalysts.<sup>54</sup>

Metals like platinum (Pt) is considered to be one of the ideal candidates for the electrode of these sensors. The Pt surface allows glucose oxidation by losing two electrons in the process.<sup>55</sup> However, the sensing capability of Pt-based sensors is hindered by two main problems. Firstly, the adsorption of Cl ions and intermediates can dramatically poison Pt-based catalysts' activity by rapidly covering the electroactive surfaces. Secondly, due to the electrocatalytically active nature of Pt, it can oxidize many other undesired small molecules, which affects the selective detection of the desired entity.<sup>56</sup> Researchers have been trying to work on alternatives

to pure metal electrodes like nanocomposite materials to overcome these problems. Since the sensitivity of these sensors depends upon the morphology and active surface area of electrodes, the electrode surface modification can be done by deposition of nano-structured materials.<sup>50,57</sup> For example, the electrodeposition process used Pt nanostructures to cover the bare Pt electrodes.<sup>57</sup> The size and shape of Pt nanostructures were controlled by deposition parameters and the ratio of reactants. With the smaller Pt nanostructures, the electroactive surface areas increase by two orders of magnitude. Also, the Pt nanostructures show remarkable electrocatalytic activity towards glucose oxidation. Many other studies have also been performed to improve the selectivity, response time, and detection limit using Pt nanostructures, which makes it a potential candidate for glucose sensing.<sup>58–60</sup>

Along with pure metals, transition metal-based oxides also received much attention because of their stable nature under ambient conditions. Metal-oxides and their complexes have been widely explored.<sup>54,61</sup> Nanoscale metal oxide materials differ dramatically from their bulk counterparts in terms of their properties. Also, the fabrication is cost-effective and straightforward, along with an enhanced surface area and higher crystallinity, which contributes to higher sensitivity towards glucose sensing.<sup>62</sup> For example, recently, a cost-effective glucose sensor based on electroplated copper using laser radiation on top of carbonated flexible meta-polyaramid has been reported.<sup>61</sup> Later, these films were annealed in an ambient environment, resulting in dispersed CuO urchins and Cu microspheroids. A higher sensitivity of Cu/CuO micro-nanostructures was found towards glucose. A higher amperometric sensitivity was found for CuO urchins of the order of  $0.39 \text{ mA cm}^{-2} \text{ mM}^{-1}$  in the glucose concentration range of  $1 \text{ } \mu\text{M}$  to  $3 \text{ mM}$ . Also, it was found that after amperometry testing, the chemical composition of CuO urchin remained unchanged, which makes it repeatable and reusable. This study is one of the examples of the development of reliable and durable sensing based on metal oxide composites, tailored shape, and the possibility of integration in flexible carriers.

### 3.2 Optical glucose sensing

The optical sensor presents a promising platform for glucose sensing, especially for non-invasive measurement. Unlike electrochemical-based biosensors, optical sensors mainly depend on the detection of photons rather than electrons.<sup>23</sup> Compared with other technologies, the optical sensor receives more attention on continuous quantification of glucose in biofluids since they can be fabricated as continuous real-time monitoring, label-free, electromagnetic-interference-free, and internally calibrated glucose monitoring systems.<sup>35</sup>

Seven leading optical technologies will be involved in this section. Some of them are spectroscopic approaches, including NIR, MIR, Raman, and PA sensing. They directly



determine glucose concentration *via* the interaction between the different wavelengths of light and the glucose molecule. The other three technologies use indirect methods to indicate the concentration of glucose. The fluorescence optical sensor utilizes fluorophores and reactants that can reversibly bind with glucose molecules to display optical signals for various glucose concentrations. Systems using OCT measure the scattering characteristic changes in subcutaneous tissue or the skin surface that correspond to the glucose concentration.<sup>17</sup> The last technology, holographic sensing, transfers glucose concentration to colorimetric information *via* diffraction caused by the stretch of the substrate synthesized with a glucose-sensitive agent. Other optical sensing technologies, such as rotating optical measurement and photothermal deflection spectroscopy, were also explored for glucose monitoring.<sup>63–65</sup> But they will not be discussed due to limited research groups or relatively old studies on them. Instead, the following sections will introduce the technical aspects for the mentioned seven technologies and their research status and limitations. Table 2 summarizes the research results and relevant characteristics of most of these detection systems.

**3.2.1 Near-infrared (NIR) spectroscopy.** NIR spectroscopy techniques are commonly used and easily accessible in analytical labs. They rely on the absorption and scattering caused by molecular vibrations and rotation of bonds inside the molecule.<sup>16</sup> The applied wavelength is in the range of 780–2500 nm (14000–4000  $\text{cm}^{-1}$ ), while the first overtone (1500–1800 nm) and the combination band (2050–2100 nm) are mostly used in non-invasive measurement.<sup>16,17</sup> For example, for aqueous glucose NIR spectroscopy measurement, the first overtone (6500–5500  $\text{cm}^{-1}$ ) and the combination (5000–4000  $\text{cm}^{-1}$ ) regions are usually applied, which are the vibration region for bending and stretching of C–H and O–H bonds.<sup>87</sup>

Transmittance and reflectance modes are the two basic measurement modes for glucose detection. Fig. 5 presents the schematic diagram for them.<sup>16</sup> In the transmittance mode (Fig. 5B), the sample is irradiated by polychromatic light from the light source (tungsten halogen or LED). The transmitted radiation is separated into its constituent wavelengths by a diffraction grating on the other side. Then sensing and analysis of the optical information is conducted using a detector and computer, respectively. The reflectance mode (Fig. 5A) is similar to the transmittance mode, but the diffraction grating is at the same side as the light source to ensure that the light can be reflected at a certain angle. Transmission spectroscopy is widely used for aqueous solutions, while for non-invasive measurement, reflectance spectroscopy is required. Moreover, it is estimated that the optical path length for transmission mode is in the range of 0.5–5 mm,<sup>88</sup> while for reflectance spectroscopy measurement is in the range of 0.4–10 mm since the light is required to penetrate through the upper layer of skin.<sup>89–91</sup>

*In vitro* NIR glucose measurement studies focus on transmission spectroscopy detection in biofluids, such as

plasma,<sup>93</sup> whole blood, and urea.<sup>66,94</sup> Their RMSEP can be concluded from 9  $\text{mg dl}^{-1}$  to 45  $\text{mg dl}^{-1}$ .<sup>17</sup> For instance, Goodarzi *et al.* reported that NIR detection for glucose could be measured down to 36  $\text{mg dl}^{-1}$  (2 mM) in solution with urea and sodium D-lactate, and the lowest RMSEP was 10.1  $\text{mg dl}^{-1}$  (0.56 mM).<sup>66</sup> Ryckeboer *et al.* proposed another approach for sensing aqueous glucose concentration.<sup>67</sup> They creatively measured glucose on a silicon chip by waveguide-based absorption spectroscopy of 1540–1610 nm. It offered a promising result with an RMSEP of 20.5  $\text{mg dl}^{-1}$  (1.14 mM) in the glucose concentration between 18 and 684  $\text{mg dl}^{-1}$  (1–36 mM).

The application of NIR spectroscopy technology in non-invasive glucose sensing has attracted more research groups. For example, in the study conducted by Olesberg *et al.*, glucose concentrations of a rat's back skin were monitored by a fiber probe with the detection range of 90–630  $\text{mg dl}^{-1}$  (5–35 mM) and SEP of 35.6  $\text{mg dl}^{-1}$  (1.98 mM).<sup>68</sup> In addition to animal trials, the NIR spectroscopy technology for glucose sensing has also reached the stage of clinical studies in various research reports. For example, Maruo and his group provided a non-invasive NIR-based sensor for diabetic patients compared to healthy people.<sup>69</sup> Five healthy and seven diabetic human subjects were involved, and the SEP was 27.2  $\text{mg dl}^{-1}$ , which was obtained under 50–500  $\text{mg dl}^{-1}$  glucose concentration. Fig. 5C illustrates the results for the comparison between predicted and referenced glucose values, as well as the CEG analysis. In 2015, they followed up with a demonstration for establishing a non-invasive model according to Beer–Lambert's law rather than using chemometrics.<sup>95</sup> In the same year, Mohammadi *et al.* reported a minimally invasive NIR CGM system using microdialysis of ISF and tested it on six T1D patients.<sup>70</sup> The result shows a mean ARD of 8.5% with the glucose concentration in the range of 60–350  $\text{mg dl}^{-1}$ .

However, there is currently no glucose sensing device based on NIR technology in the market. Arnold and Small demonstrated that NIR spectroscopy parameters, including the path length, degrees of freedom, selectivity, spectral range, and variance, could significantly influence the comparability of non-invasive glucose monitoring studies. This might bring difficulties for a reader to collect data if researchers didn't consider these parameters in their experiments.<sup>90</sup> In addition, it is challenging for NIR-based glucose sensors to reproduce similar results under different local skin environments, such as sunburn, sweating, or area with tattoos. Therefore an exploration of calibration models is required to detect various physiological states between patients.<sup>17</sup> Moreover, another problem could be the interference between the glucose spectrum and similar absorption spectrum of other molecules, such as lactate and urea (Fig. 5D).<sup>87</sup> Broad and overlapped peaks may lead to a relatively weak signal which makes it difficult to achieve accurate detection of low glucose concentration.

**3.2.2 Mid-infrared (MIR) spectroscopy.** MIR spectroscopy relies on the same absorption principle and system configuration as the NIR spectroscopy system but uses light in



Table 2 Summary of optical measurements for glucose monitoring

Measurement method	Wavelength	Research stage and type	Glucose detection range	Accuracy	Measurement site/solution	Reference
Transmission NIR spectroscopy	Combinational band and first overtone	<i>In vitro</i>	36–540 mg dl <sup>-1</sup> (1–30 mM)	RMSEP down to 10.1 mg dl <sup>-1</sup> (0.56 mM)	Aqueous solutions and serum solutions	66
Transmission NIR spectroscopy	First overtone	Prototype <i>in vitro</i> , aimed at <i>in vivo</i> invasive	18–684 mg dl <sup>-1</sup> (1–36 mM)	RMSEP of 20.5 mg dl <sup>-1</sup> (1.14 mM)	Aqueous solutions	67
Transmission NIR spectroscopy	2–2.5 μm	<i>In vivo</i> , non-invasive	90–630 mg dl <sup>-1</sup> (5–35 mM)	SEP of 35.6 mg dl <sup>-1</sup> (1.98 mM)	Skin fold, rat	68
Diffuse reflectance NIR spectroscopy	First overtone	<i>In vivo</i> , non-invasive	50–500 mg dl <sup>-1</sup>	SEP of 27.2 mg dL <sup>-1</sup>	Forearm skin, human	69
Transmission NIR spectroscopy combined with microdialysis (LEDs)	1300, 1450, 1550 nm	Prototype, invasive	60–350 mg dl <sup>-1</sup>	Mean ARD 8.5%	Forearm skin, human	70
ATR MIR spectroscopy, FTIR source		<i>In vitro</i>	36–482 mg dl <sup>-1</sup>	RMSEP of 10.4 mg dl <sup>-1</sup>	Blood plasma	71
Transmission MIR spectroscopy	1230–1030 cm <sup>-1</sup>	<i>In vitro</i>	Approx. 20–140 mg dl <sup>-1</sup>	RMSEP of 6.9 mg dl <sup>-1</sup>	Blood serum	72
Back-scattered MIR spectroscopy	8–10 μm	<i>In vivo</i> , non-invasive	80–160 mg dl <sup>-1</sup>	84% of measurements in zone A of CEG	Skin fold of the hand, human	73
Transmission MIR spectroscopy	9.7 μm	<i>In vivo</i> , minimally invasive	Approx. 75–600 mg dl <sup>-1</sup>	Median ARD 11.0%	Transcutaneous skin, rats	74
ATR MIR spectroscopy, FTIR source	Peak around 1155 cm <sup>-1</sup>	<i>In vivo</i> , non-invasive	Approx. 75–175 mg dl <sup>-1</sup>	Measurement errors less than 20%, R <sup>2</sup> = 0.75	Lip mucosa, human	75
Raman spectroscopy in reflection mode	785 nm	<i>In vitro</i>	38–775 mg dl <sup>-1</sup>	RMSEP of 22 mg dl <sup>-1</sup>	Aqueous humor of the eye, human	76
Transmission Raman spectroscopy	830 nm	<i>In vivo</i> , non-invasive	75–320 mg dl <sup>-1</sup>	R <sup>2</sup> = 0.81, RMSEP of 16.8 mg dl <sup>-1</sup>	Thenar skin fold of the hand, human	77
Transmission Raman spectroscopy	830 nm	<i>In vivo</i> , non-invasive	100–460 mg dl <sup>-1</sup> (5.6–25.6 mM)	RMSEP approx. 27–36 mg dl <sup>-1</sup> (1.5–2 mM)	Ear, dog	78
Surface-enhanced Raman spectroscopy	785 nm	<i>In vivo</i> , minimally invasive	31–600 mg dl <sup>-1</sup>	100% of measurements in zone A & B of CEG	Subcutaneous, rats	79
Photoacoustic spectroscopy	Dual-wavelength scheme around 1100 cm <sup>-1</sup>	<i>In vivo</i> , non-invasive	90–170 mg dl <sup>-1</sup>	R = 0.8	Arm skin, human	80
Photoacoustic spectroscopy	1220–1000 cm <sup>-1</sup>	<i>In vivo</i> , non-invasive	40–250 mg dl <sup>-1</sup>	100% of measurements in zone A & B of CEG	Arm skin, human	21
Fluorescence sensing		Prototype, minimally invasive	100–350 mg dl <sup>-1</sup>	Mean ARE 13%	Subcutaneous on arm, human	81
Fluorescence sensing		Prototype, minimally invasive	60–370 mg dl <sup>-1</sup>	Mean ARD 8.3% on arm, 11.4% on the abdomen	Subcutaneous on arm and abdomen	82
Fluorescence sensing		Product, invasive	40–400 mg dl <sup>-1</sup>	Mean ARD 11.1%	Implanted subcutaneously	24
Optical coherence tomography	1300 nm	<i>In vivo</i> , non-invasive	110–400 mg dl <sup>-1</sup>	R = 0.88	Ear, rabbit	83
Optical coherence tomography	1310 nm	<i>In vivo</i> , non-invasive	98–442 mg dl <sup>-1</sup>	Mean ARD 11.5%	Skin, human	84
Holographic sensing	500–700 nm (visible light)	<i>In vitro</i>	54–594 mg dl <sup>-1</sup> (3–33 mM)	100% of measurements in zone A & B of CEG	Blood plasma, human	85
Holographic sensing, a laser pulse with 532 nm	510–1100 nm	<i>In vitro</i>	3.6–7200 mg dl <sup>-1</sup> (0.2–400 mM)	R = 0.79	Urine, human	86

the region of 4000–400 cm<sup>-1</sup> (2.5–25 μm). 4000–1000 cm<sup>-1</sup> (2.5–10 μm) is more commonly applied for daily measurement. Besides the overlap with strong water absorption peaks around 3000 cm<sup>-1</sup> and 1400 cm<sup>-1</sup>, the absorbance in the 1200–1000 cm<sup>-1</sup> region is specific for glucose molecules. Fundamental

molecular vibrations define the absorption of MIR spectroscopy. Therefore, compared with NIR spectra, MIR spectra have shaper bands, showing higher selectivity and stronger signals.<sup>17</sup>

Most available studies in glucose detection rely on transmission MIR spectroscopy for subcutaneous



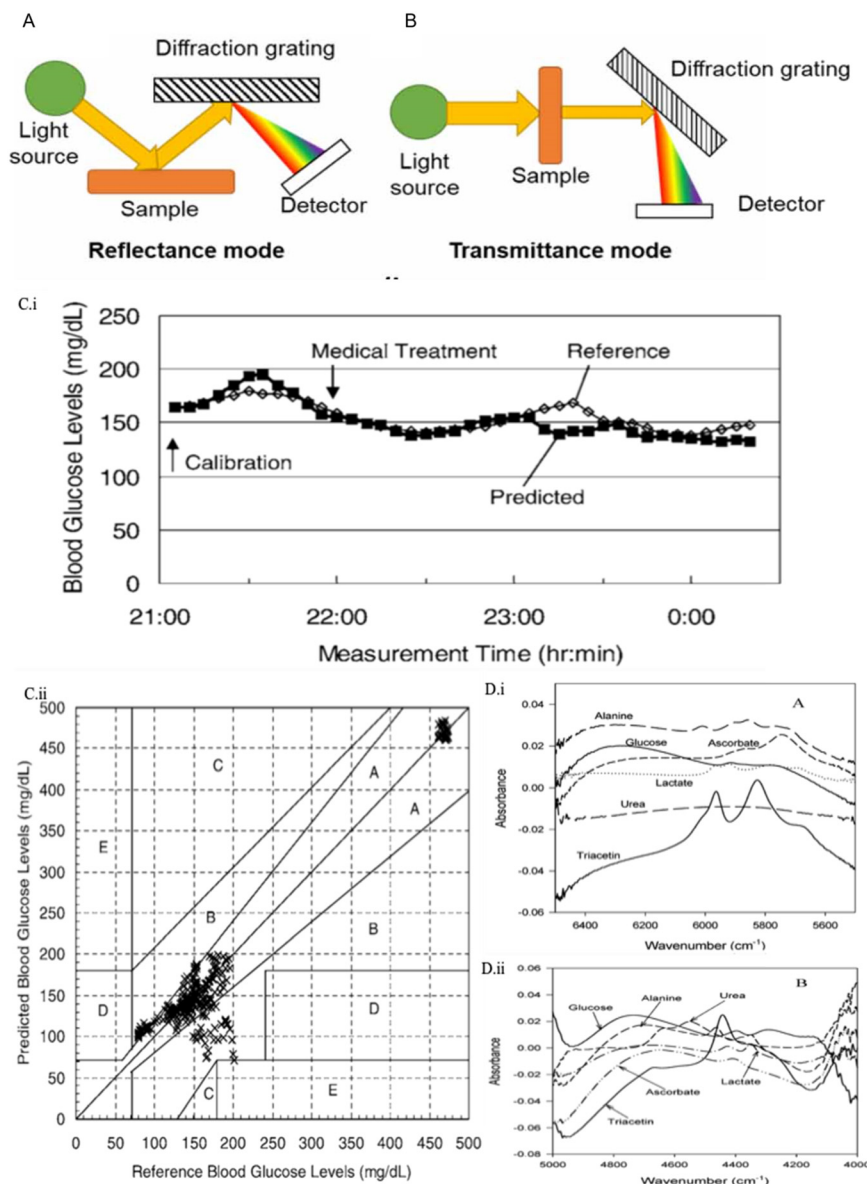


**Fig. 5** NIR spectroscopy techniques in glucose sensing. (A) Schematic representation for transmittance NIR spectroscopy. (B) Schematic illustration for reflectance NIR spectroscopy.<sup>92</sup> Reproduced from ref. 92 with permission from IOPScience, Copyrights 2021. (C) Results for non-invasive NIR-based glucose sensors.<sup>69</sup> (i) A time course chart for the subjects with the best agreements between the predicted and reference blood glucose levels. (ii) Correlation between the reference and predicted blood glucose levels in the same experiment stage with the Clarke error grid. 80.3% of data are in the A zone, 19.7% are in the B zone, and 0% are in the C, D, and E zones. Reproduced from ref. 69 with permission from Society for Applied Spectroscopy, Copyrights 2006. (D) NIR absorbance spectra of glucose, lactate, urea, alanine, ascorbate, and triacetin.<sup>87</sup> (i) Spectra in the first overtone region. (ii) Spectra in the combination region. Reproduced from ref. 87 with permission from ACS, Copyrights 2004.

measurements or non-invasive measurements using reflectance spectroscopy. MIR sources for subcutaneous measurement are required to be robust due to the strong absorption of water in tissue which limits the MIR signal to penetrate more than 0.1 mm in tissue. The quantum cascade laser (QCL) is developed for such a high-energy source. It is a semiconductor laser that can be customized to a specific single wavelength or tuned within the desired wavelength range. For CGM, attenuated total reflectance (ATR) spectroscopy, as shown in Fig. 6A, can also be used for non-invasive measurements.<sup>96</sup> In ATR-MIR spectroscopy, total

internal reflection occurs in the ATR crystal area in contact with the sample, thereby guiding the light transmission direction. At the same time, the evanescent field of light extends into the sample. Light is detected when it comes out of the crystal, and the absorption spectrum is determined by the evanescent light absorbed by the sample.

MIR spectroscopy has been applied for the quantification of glucose in artificial and *in vitro* biofluids. In the early research stages, the Heise group confirmed that glucose concentration under physiological conditions could be predicted *via* ATR-MIR spectroscopy using Fourier transform



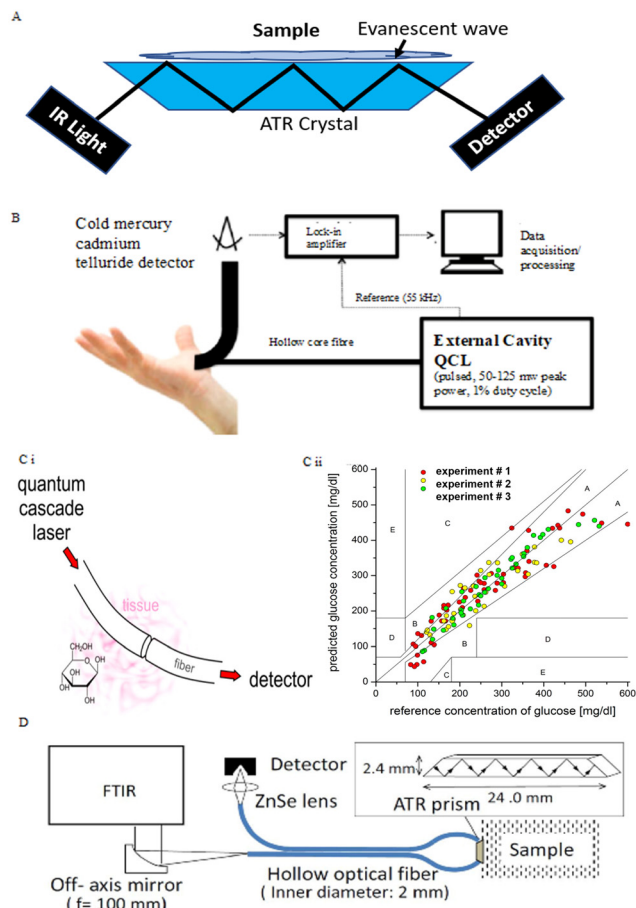


**Fig. 6** MIR spectroscopy techniques in glucose sensing. (A) Schematic for ATR spectroscopy. Light can undergo multiple internal reflections in the crystal with a high refractive index. The evanescent light resulting from this can extend into the sample which is in contact with the crystal. The absorption of this evanescent wave is used to construct an MIR absorption spectrum. Adopted from ref. 17. (B) Setup for collecting MIR spectra of human hand's skin. The hollow-core fiber transmits light from the QCL and collects backscattered light from the inside of the skin. The optical transmission wavelength is 8–10  $\mu\text{m}$ .<sup>73</sup> Reproduced from ref. 73 with permission from optical Publishing Group, Copyrights 2014. (C) MIR system with a single wavelength of the QCL.<sup>74</sup> (i) Simple schematic for light going through the subcutaneous fiber and being received by the detector. (ii) Comparison of glucose values for reference BGL measured by a test strip and glucose concentration predicted by the *in vitro* MIR analysis of ISF at the same time. Reproduced from ref. 74 with permission from ACS, Copyrights 2014. (D) Experimental setup and dimensions of an ATR prism.<sup>75</sup> Light emitted by the FTIR with a frequency of 100 mm and transferred in the hollow optical fiber reflects multiple times with a high refractive index in an ATR prism connected to the sample. The optical signal is collected by the detector via a ZnSe lens. Reproduced from ref. 75 with permission from Optical Publishing Group, Copyrights 2016.

infrared (FTIR) spectrometers based on silver halide fibers.<sup>71</sup> Results offered an RMSEP of 10.4 mg dl<sup>-1</sup>. Another study conducted by Brandstetter *et al.* focused on the highly accurate glucose measurement in human serum samples by

using a QCL as the infrared source.<sup>72</sup> The RMSEP = 6.9 mg dl<sup>-1</sup>, and the experimental glucose concentration range was approximately 20–140 mg dl<sup>-1</sup>. These two studies investigated broad wavelength ranges in MIR spectroscopy and used multivariate data analysis to extract relevant information. For CGM, if the same principles are applied, the use of tunable MIR lasers is necessary, but they are too large and expensive for a point-of-care personal device.

Several research groups have explored the use of MIR spectroscopy for non-invasive glucose measurement by using a QCL or FTIR as the light source. In the studies for CGM by using MIR spectroscopy, the QCL is usually used in a specific narrow wavelength range to provide accurate concentration prediction. In the studies from the Gmachl group, they measured the back-scattered light from the skin between the forefinger and thumb by using non-invasive MIR-based measurement, as shown in Fig. 6B.<sup>73</sup> Three human individuals were measured, and 84% of values of glucose concentrations were in zone A of the CEG analysis with the glucose range of 75–160 mg dl<sup>-1</sup>. In addition, an MIR system using a QCL at a single wavelength (9.7  $\mu\text{m}$ ) was developed (Fig. 6Ci), and transcutaneous fibers were used as media for light transmission in subcutaneous glucose measurement in three rat subjects.<sup>74</sup> The system offered a CGM measurement within 3 hours, down to 4 seconds between each data collection. As shown in Fig. 6Cii, glucose values for each rat experiment were in zone A and B in the CGE, giving a median ARD of 11.0% with the glucose range of 80–550 mg dl<sup>-1</sup>. Aside from QCLs, FTIR spectrometers also can be employed in non-invasive measurement with ATR-MIR analysis. Kino *et al.* reported the FTIR ATR-MIR-based glucose measurement on human lip mucosa, which used a hollow-optical fiber for light transport. The multiple internal reflections in the ATR crystal are performed under 1100  $\text{cm}^{-1}$ , as shown in Fig. 6D.<sup>75</sup> They achieved glucose measurements with errors of less than 20% and  $R^2 = 0.75$ .

One of the challenges in using MIR sensing devices is the limited depth that these wavelengths penetrate the skin. Since waves are absorbed by water in tissues, the light transmission rate is highly dependent on the individual's skin water content. Specific calibrations may be required for each measurement with different skin properties. On the other hand, the existing high energy emitting source is relatively large and expensive for personal non-invasive measurement, which leads to little attention to MIR-based glucose monitoring.

**3.2.3 Raman spectroscopy.** Raman spectroscopy depends on the rotational states and vibrational states of molecules and is used to detect specific absorption bands to identify corresponding molecules. Typical vibration modes for glucose present in the spectrum are C–H bond stretching (around 2900  $\text{cm}^{-1}$ ) and C–O bond stretching (800  $\text{cm}^{-1}$ ), as well as C–C bond stretching (300  $\text{cm}^{-1}$ ).<sup>97</sup> The single wavelength of light scatters in all directions when it hits an object, and scattered light is separated into two groups.



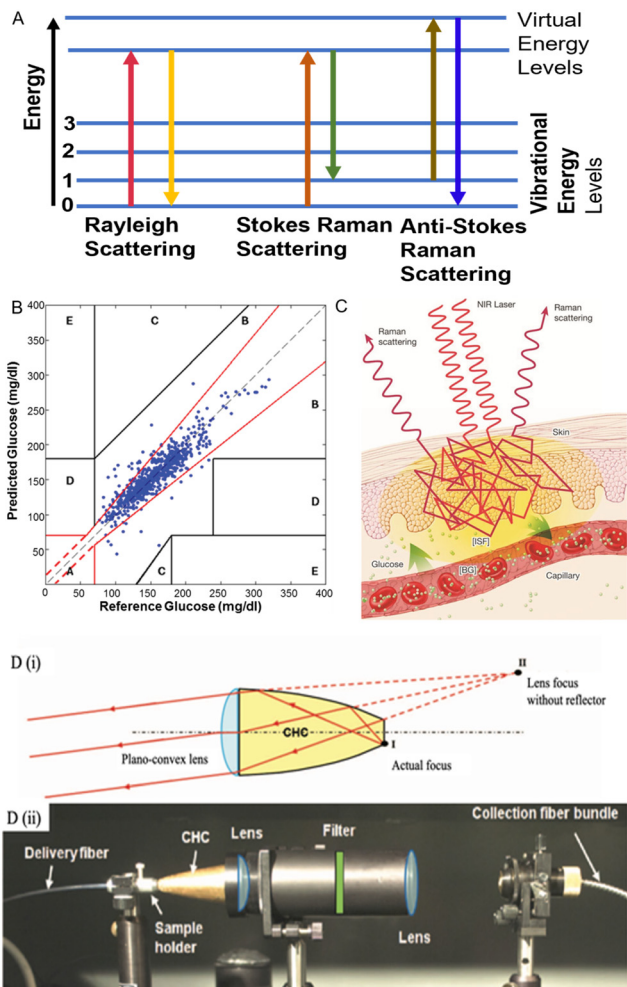


**Fig. 7** Raman spectroscopy techniques in glucose sensing. (A) Molecules change in different energies in Raman spectroscopy. Adopted from ref. 17. In Rayleigh scattering, photon energy does not change. In Stokes Raman scattering, the molecule absorbs energy, and the photon shifts to a longer wavelength, and *vice versa* for anti-Stokes scattering. (B) CGE analysis for the correlation between glucose concentrations measured by Raman spectroscopy and BGL to reference glucose concentrations measured by a finger-prick glucometer (730 data points, 18 human subjects).<sup>77</sup> Reproduced from ref. 77 with permission from *AIP Advance*, Copyrights 2011. (C) Schematic representation of Raman spectroscopy for glucose sensing.<sup>99</sup> (D) Schematic representation of the CHC setup.<sup>77</sup> (i) The principle for how CHC enhances the Raman scattering. With a focusing lens, the CHC can allow collimation while maintaining a relatively short physical length. Due to the hyperbolic shape of the reflector, light emanating from point I (the actual focus of the lens) is collimated by the lens as if it were coming from point II. (ii) A side view of the transmission mode Raman spectroscopy setup. Reproduced from ref. 77 with permission from *AIP Advance*, Copyrights 2011.

Radiation having the same wavelength as the incidence light is called Rayleigh scattering (elastic scattering), and the rest of the radiation with a different wavelength is termed Raman scattering (inelastic scattering).<sup>16</sup> The difference in wavelength between Raman scattering and Rayleigh scattering is the Raman shift, which is shown as the energy difference between the molecule's initial and final vibrational

states, as shown in Fig. 7A.<sup>17,98</sup> In Raman scattering, small energy is transferred between a molecule and a photon. Molecules can absorb or release energy which are represented as the process of Stokes Raman scattering and anti-Stokes Raman scattering, respectively. Fig. 7C illustrates the basic configuration of a Raman spectroscopy system. A single wavelength of light, such as visible or NIR light, is sufficient for a Raman spectrometer to measure the frequency shift, which facilitates the wide application of this technology.

Raman spectroscopy has attracted great attention in non-invasive CGM development in the last few decades. Both *in vitro* and *in vivo* were explored. In the study conducted by the Pelletier group,<sup>76</sup> Raman-based glucose measurement of *in vitro* human aqueous humor was reported, and the results were correlated. Results correlate blood and humor glucose concentration with RMSEP = 22 mg dl<sup>-1</sup> (measured glucose levels: 38–775 mg dl<sup>-1</sup>). Compared with blood, the composition of human aqueous humor is relatively simple, which means that there are fewer absorption peaks that can lead to interference in the Raman spectrum. This provides advantages for glucose detection. In addition, Raman spectroscopy also can be used to measure glucose levels through the skin. Kong *et al.* developed a novel portable Raman spectroscopy system in transmission mode with non-imaging optics designed to enhance the light collection. As represented in Fig. 7D, the non-imaging optical unit is termed compound hyperbolic concentrator (CHC). The system was applied on the hand's thenar skin fold, and 18 human subjects were involved in this clinical experiment. Results presented a good correlation with the Raman spectra predicted glucose level and that of finger-prick measurement. All collected data were in the zone A and B of the CEG analysis (Fig. 7B) and RMSEP = 16.8 mg dl<sup>-1</sup>. Afterward, Shih *et al.* applied the same transmission Raman spectroscopy system on ears in a dog model and also achieved good results with RMSEPs of approximately 27–36 mg dl<sup>-1</sup> (1.5–2 mM) in the glucose range of 100–460 mg dl<sup>-1</sup> (5.6–25.6 mM).<sup>78</sup>

Raman spectroscopy was also used to support the research in minimally invasive glucose measurement. For example, Ma *et al.* reported a minimally invasive glucose measurement sensor detected by a surface-enhanced Raman scattering (SERS) chip subcutaneously implanted in rats.<sup>79</sup> Six individual subjects were involved, and the measurement was performed 17 days after chip implantation, from which only one calibration was demonstrated. In CEG analysis, 100% measurements from all subjects were in zone A and B, and the RMSEP = 13.7 mg dl<sup>-1</sup> when the glucose concentration is lower than 80 mg dl<sup>-1</sup> with a collection time of 2 minutes. The main limitation for Raman spectroscopy is the small scattering cross-section, which may interfere with the Raman scattering signal. In addition, long acquisition times are required for good signal detection. Problems of biocompatibility and potential toxicity of the Raman enhanced chip substrate need to be considered in the actual clinical application of this technology.



**3.2.4 Photoacoustic (PA) spectroscopy.** PA spectroscopy is a kind of acoustic detection *via* the measurement of the energy effect of light absorption. During PA imaging, light generated by short laser pulses with a single wavelength is introduced into tissue which absorbs parts of the energy by specific molecules, thereby inducing microscopic localized heating.<sup>100</sup> The amount of absorbed heat is determined by the heat capacity of the examined tissue. The volumetric expansion resulting from the heat could generate an ultrasound wave detected in a photoacoustic cell by a piezoelectric transducer (microphone) that can sense acoustics or pressure. The electrical signal is further amplified and sent to the computer for analysis. Glucose concentration in blood or ISF can be quantified *via* tracking detected variations in the signal from peak to peak. The light was emitted by a QCL and touches the sample to generate ultrasound waves. The MIR source is usually introduced in PA spectroscopy, such as QCLs or FTIR since they can be set to particular wavelengths that target MIR glucose absorption bands to selectively detect glucose.<sup>17</sup> The acquisition time of PA spectroscopy is very short (as low as

seconds), which is only caused by the scanning time of the light source.

Glucose monitoring devices using PA spectroscopy were developed for non-invasive measurement by several research groups. Pleitez *et al.*, a German group, developed an MIR-based PA spectroscopy system for glucose monitoring *in vivo* non-invasive measurement in the human epidermis.<sup>21</sup> QCLs with 1000–1200  $\text{cm}^{-1}$  wavelengths were used as the light source to focus on skin, and the absorbed acoustic waves were detected in a gas cell coupled to the skin. The representation of the setup is shown in Fig. 8A. Measurements were performed on three diabetic volunteers during an OGTT. The glucose concentration was measured from 40  $\text{mg dl}^{-1}$  to 250  $\text{mg dl}^{-1}$  during the process. Results for PA spectra of non-invasive ISF glucose levels are presented in Fig. 8B. The PA spectra illustrated clear signals for glucose identification and 100% measurements in the zone A & B of CEG analysis. Another research performed by the Kottmann group used a similar PA spectroscopy system. They reported a small PA platform that could offer precise measurements for ISF glucose levels in the range of 90–180  $\text{mg dl}^{-1}$  with  $R^2 =$

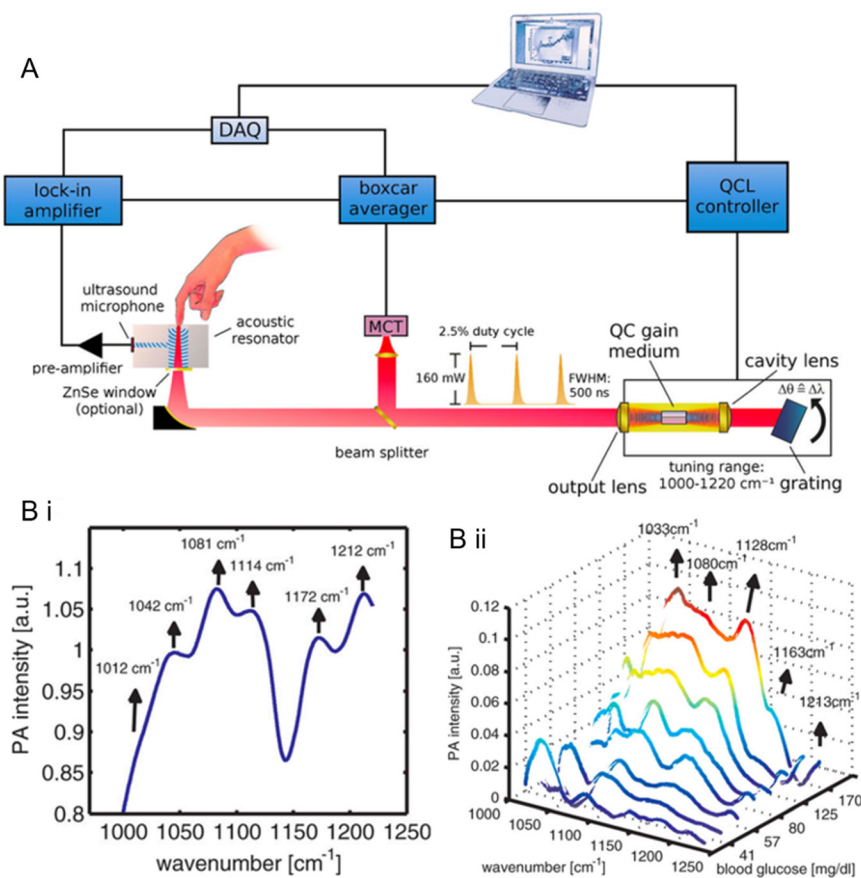


**Fig. 8** (A) A representation of the optical setup and schematic signal processing for the photoacoustic (PA) measurement of human subcutaneous glucose.<sup>21</sup> (B) PA imaging spectra.<sup>21</sup> (i) PA spectrum of human skin in the glucose fingerprint region (1000–1200  $\text{cm}^{-1}$ ). The central peak wavenumbers correspond to the vibration frequencies of lipid layers and corneocytes. (ii) Variation of the PA spectra of the subject during an oral glucose tolerance test (OGTT). The BGL rose from 37 to 237  $\text{mg dl}^{-1}$ . The background matrix was subtracted to provide the correct spectrum. The absorption features of glucose can be observed as the glucose concentration in blood increases. Reproduced from ref. 21 with permission from ACS, Copyrights 2013.



0.8.<sup>80</sup> They combined two QCLs with different wavelengths and the PA spectroscopy system to enhance the accuracy. However, from experimental data, the best performance of this PA cell was observed under N<sub>2</sub> condition, which could stabilize the humidity conditions of sample cells, and this is not feasible for portable personal CGM devices.

There is currently no commercialized PA imaging-based glucose sensor. The main challenge for PA glucose monitoring is the weak signals for targeted glucose absorption bands which were either NIR absorption bands or MIR absorption bands.<sup>17</sup> Although the MIR light source could offer relatively stronger signals compared with NIR, the large FTIR spectrometer and expensive QCLs minimized the possibility of developing a portable and cost-effective PA-based glucose sensor.

**3.2.5 Fluorescence sensing.** The fluorescence principle relies on the light emission from a molecule that absorbs energy at a specific wavelength from incidence radiation and is excited from the ground state to a higher energy level.<sup>17,101</sup> Fluorophores, as media in fluorescence technology, could emit fluorescence with specific characteristics proportional to the concentration of the analyte to be measured, and they could be fabricated with desired properties in actual application. Fluorescence sensing measures with high sensitivity can be applied in affordable light sources, such as LEDs generating ultraviolet (UV) or visible light, which has aroused great interest in developing clinical glucose sensors. Although glucose itself is fluorescence whose intensity is related to the glucose concentration, few researchers focus on the direct glucose fluorescent property for CGM due to its low selectivity, irreversibility, and issues with interference signals.<sup>16</sup> Instead, intermediary molecules termed as receptors play the role of label in fluorescence glucose sensing. They could be engineered to reversibly bind with glucose molecules in a more effective approach, causing altered fluorescence.<sup>102</sup> In this case, an exogenous fluorophore must be introduced into the sample, and the fabricated fluorophore should only fluoresce with the presence of glucose molecules, as illustrated in Fig. 9A. As the glucose concentration increases, a stronger fluorophore intensity will appear, which indirectly quantifies the glucose concentration. Different types and properties of receptors were reported for fluorescence-based glucose measurements, including boronic-acid derivatives, enzymes, glucose binding proteins (like concanavalin A (ConA)), carbon nanotubes and quantum dots.<sup>25,100,103–105</sup>

Fluorescence sensing has been studied for glucose monitoring in both biofluids and subcutaneous measurements. Several research groups have worked on optical sensors based on fluorescence detection, and it was confirmed to be highly sensitive for glucose determination in human serum.<sup>106,107</sup> On the other hand, fluorescence sensing has been of great interest in non-invasive glucose measurement since small fluorescence-based devices are relatively accessible, affordable, and easily implanted under the skin without surgery.<sup>104</sup> Several studies focused on

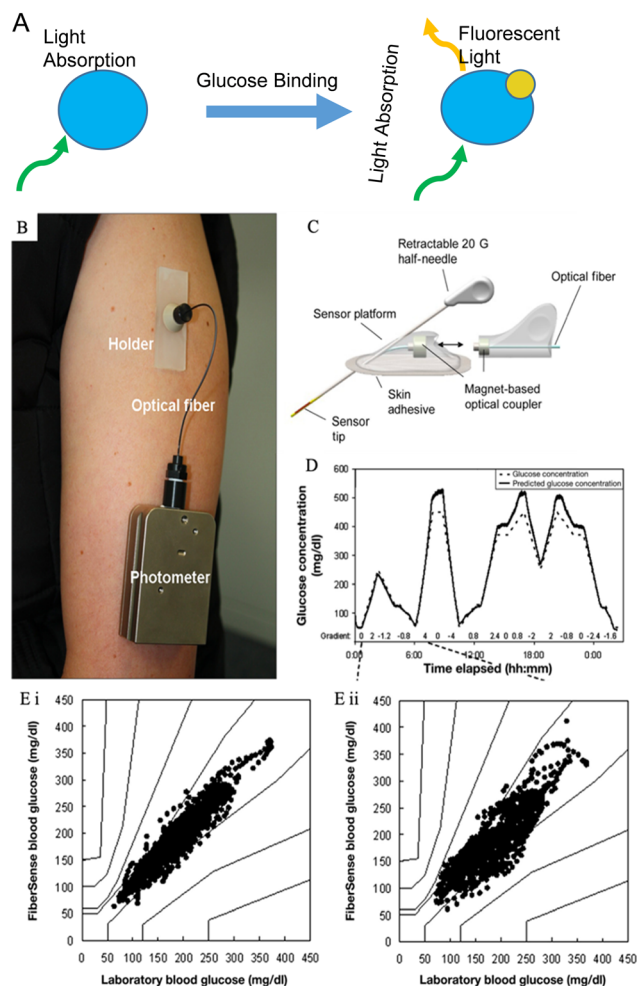


**Fig. 9** Fluorescence sensing for glucose monitoring. (A) The glucose sensing process *via* fluorescent labeling. Adopted from reference ref. 17. The blue molecule represents the engineered fluorophore, and the yellow molecule is the glucose. Fluorescent light only emits under the existence of glucose molecules. (B) A photograph of the FiberSense CGM sensor worn on the upper arm.<sup>82</sup> Reproduced from ref. 82 with permission from Diabetes Technology Society, Copyrights 2013. (C) Schematic representation of a first-generation FAS.<sup>81</sup> Reproduced from ref. 81 with permission from Diabetes Technology Society, Copyrights 2012. (D) Kinetics of the FiberSense CGM system.<sup>82</sup> The predicted glucose concentration line largely matches the reference glucose concentration. (E) PEG analysis of the measurements on FiberSense CGM.<sup>82</sup> (i) Upper arm data analysis; (ii) abdomen data analysis. 100% measurements in both sites were in zone A and B in PEG. Reproduced from ref. 82 with permission from Diabetes Technology Society, Copyrights 2013.

developing contact lens glucose sensors in the past decades.<sup>108,109</sup> Meanwhile the challenges are that the correlation between BGL and glucose levels in tear fluids is still not proved by enough evidence, and the low concentration of glucose in tear fluids brings difficulties for accurate measurement. Significant results have been achieved in using fluorescence-labeled ConA as an indicator fluorophore for glucose concentration quantification. In 1979, Schultz *et al.* firstly introduced a fluorescence-based subcutaneous glucose sensor that used ConA as the



carbohydrate receptor.<sup>110</sup> They further developed this sensor system, and BioTex Inc is currently studying it, with the name Fluorescence Affinity Sensor (FAS). Fig. 9C presents the schematic of the FAS. The FAS utilized fluorescence-labeled ConA as the fluorophore, placed in a hollow dialysis fiber connected to an optical fiber. The detection principle is based on the competitive binding between glucose with ConA and dextran with ConA. When glucose binds with ConA, it displaces dextran, resulting in a fluorescent signal proportional to the glucose concentration. Dutt-Ballerstadt *et al.* reported a pilot study on human using the FAS and the results presented a good correlation between the sensor predicted glucose value and the reference values with an ARE = 13%.<sup>81</sup> Another research group developed a similar fluorescence-based glucose sensor for CGM and conducted clinical trials.<sup>82</sup> This sensor is named FiberSense, and the patent belongs to Eversense GmbH, Grossostheim (Germany). As shown in Fig. 9B, FiberSense could be placed on the human upper arm or abdomen for real-time glucose monitoring, and it also used ConA as the receptor. In the clinical study, the FiberSense CGM sensor was implanted in both arm and abdomen sites to monitor glucose levels for 3 hours on six human subjects. Fig. 9D and E present the

performance of the FiberSense CGM system, and results showed that the overall mean ARD equals 8.3% for upper arm sensors and 11.4% for abdomen sensors. Few data in the hypoglycaemic range were collected, and the sensor needed a finger-prick calibration once per day.

Moreover, in 2016, the Eversense CGM system was released by Senseonics (an American company) in the European market. Eversense is the only commercialized available wearable CGM device based on optical measurement and this system used a boronic-acid derivative as the fluorescent indicator. The mean ARD of the Eversense CGM system is 11.1%.<sup>24</sup>

Although fluorescence sensing has been well developed for measuring glucose concentration, some limitations still exist in current research. For example, for non-invasive measurement, light scattering of fluorescence may be influenced by different skin properties, such as the amount of pigmentation. Besides, for minimally invasive measurement, calibration is still required in fluorescence-based CGM systems by finger-prick measurement to solve signal drift and loss of fluorophores *via* the photobleaching process in long-term use. Moreover, sugars such as galactose and fructose can bind with many fluorophores

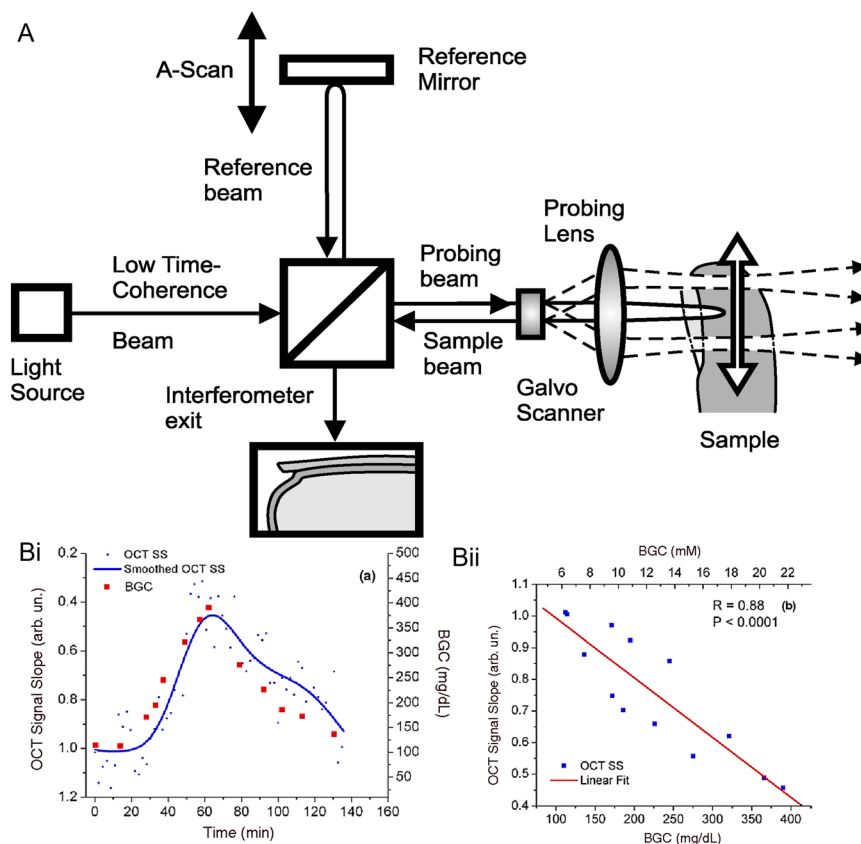


**Fig. 10** OCT technology in glucose sensing. (A) Schematic for the principle of OCT technology.<sup>112</sup> Reproduced from ref. 112 with permission from Elsevier, Copyrights 2010. The OCT system contains a light source, a reference arm, a sampling arm for backscattered light collection, a beam splitter (movable) to adjust the path length, and a photoelectric detection sensor connected to a computer for signal analysis. When the light from the two arms travels the same distance (within the coherence length), an interference pattern is generated. (B) OCT signals were obtained from rabbit ears *via* glucose injection experiments.<sup>83</sup> (i) Plots for OCT signals *versus* time. (ii) Plots for OCT signals *versus* BGL, where  $R$  is the correlation coefficient. Reproduced from ref. 83 with permission from IOP Publishing Ltd, Copyrights 2003.



that can bind with glucose, which brings interference in measurements and significantly limits the number of useful fluorophores.

**3.2.6 Optical coherence tomography (OCT).** OCT relies on the principle of coherent radiation from the low-coherence light generated by an interferometer.<sup>111</sup> It can provide micron-level high-resolution detection of changes in the optical properties of biological tissues. As shown in Fig. 10A, the glucose concentration in ISF is predicted by the light interferogram created by backscattered light from tissue and the reference light.<sup>16</sup> When the glucose concentration increases in the tissue, the refraction index of the tissue will also increase, resulting in the decrease of the scattering coefficient. The change of scattering coefficient subsequently changes the interferogram, which determines the glucose concentration.<sup>17</sup> OCT typically employs light with a wavelength between 800 and 1300 nm, which is in the NIR range. Therefore, a relatively cheap and small NIR light source could be utilized in OCT technology.

Due to the high signal-to-noise ratio and the deep penetration length, OCT technology has great promise in non-invasive glucose monitoring. Larin *et al.* reported a pilot study on non-invasive BGL monitoring with the OCT technology in animals.<sup>83</sup> New Zealand rabbit was one of the experimental subjects, and Fig. 10B shows the result of its OCT signals. On *in vivo* measurements on rabbits, the designed OCT system presented a quite good correlation with BGL and  $R = 0.8$  in the glucose detection range of 110–400 mg dl<sup>-1</sup>. In addition, they pointed out that the OCT signals may be significantly influenced by motion artifacts and the skin's temperature. Moreover, OCT technology was also explored for *in vivo* non-invasive glucose measurement on human subjects. An OCT-based glucose monitoring device was developed by the GlucoLight Company (Bethlehem, PA). In 2008, they conducted a small pilot study on this device and successfully conducted experiments on 27 diabetic patients, including 15 subjects with T2D and 12 subjects with T1D.<sup>84</sup> After two hours of measurements on each subject, the mean ARD of this device

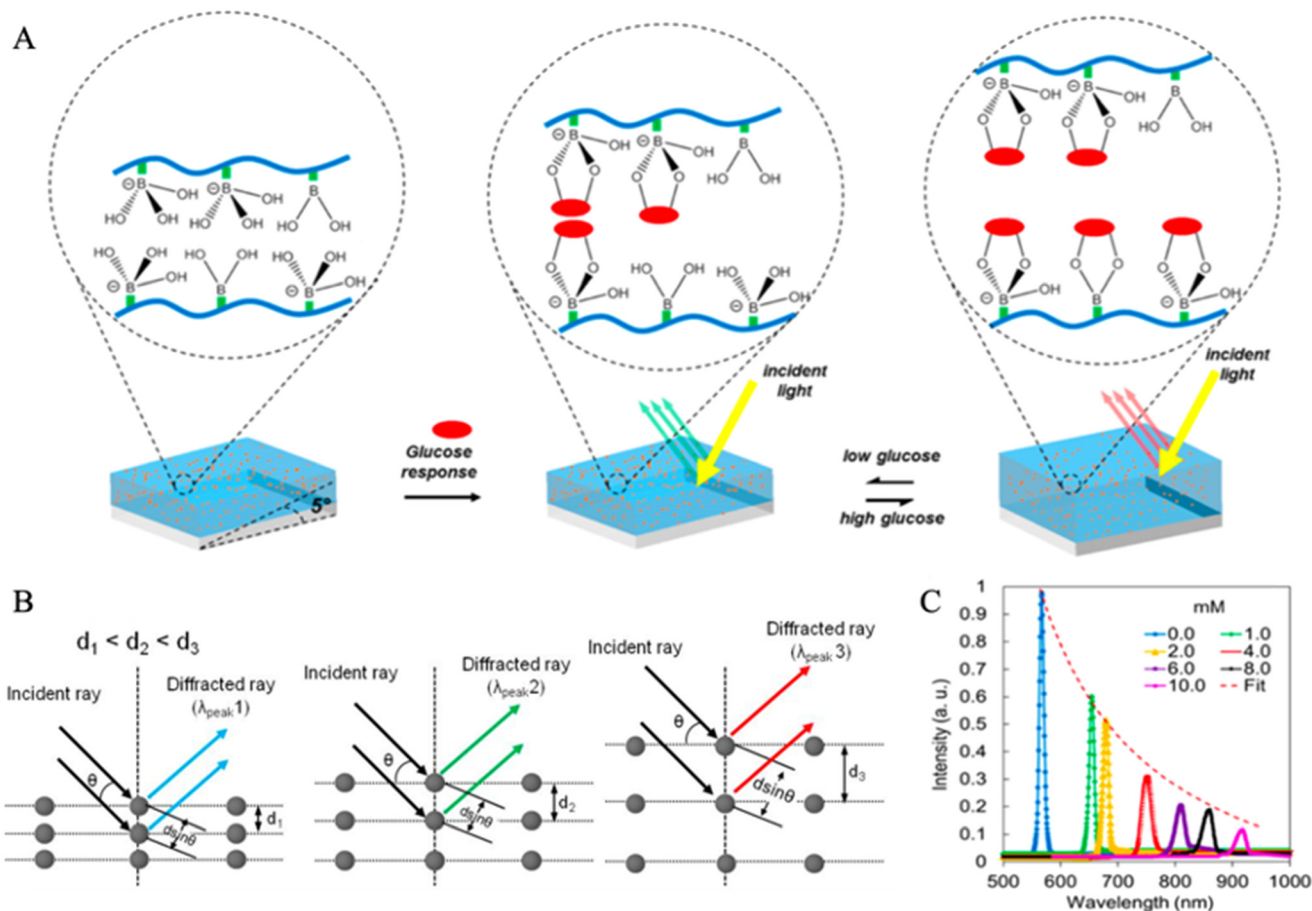


**Fig. 11** Holographic sensing for continuous glucose monitoring. (A) The schematic diagram for the generation of optical information by a 3-APB-based hydrogel hologram.<sup>86</sup> When the glucose concentration is low, the hydrogel will shrink, decreasing  $d$  and vice versa. Furthermore, the reduction of  $d$  will cause a 'blue shift' of diffracted light. Reproduced from ref. 86 with permission from ACS, Copyrights 2014. (B) Bragg's diffraction.<sup>114</sup> Bragg's diffraction is based on Bragg's law. With the increase of  $d$  spacing of a polymer layer (glucose sensing layer), the color of the diffracted ray changes from blue to green to red. This trend of wavelength change (from 500–700 nm) is called the 'redshift'. Reproduced from ref. 114 with permission from Wiley, Copyrights 2017. (C) Curves for Bragg peak shifts under different concentrations of glucose in artificial urine solutions.<sup>86</sup> With an increase of glucose concentration, the Bragg peaks will shift to longer wavelengths. The correlation between the intensity and the wavelength is also shown. Reproduced from ref. 86 with permission from ACS, Copyrights 2014.



was reported to be 11.5%. However, no concentration in the hypoglycaemic range was measured in the study, and there is no further research on this device published.

The major challenges for the OCT technique in glucose sensing are that the measured signal for the change of the scattering coefficient is relatively weak, and OCT is sensitive to many factors. Affecting factors include motion artifacts, skin properties, and the skin's environment, such as pH, temperature, and humidity.<sup>17</sup> Among them, motion artifacts can cause changes in interference patterns and skin factors that may lead to scattering coefficients. Therefore, personalized calibration is necessary for non-invasive glucose measurement based on OCT technology.

**3.2.7 Holographic sensing.** Holographic sensing is a novel technology in optical glucose sensing, which relies on the systematic diffractions generated by a narrow range of light (UV or NIR light) to detect and quantify the glucose concentration.<sup>113</sup> The three-dimensional imaging of the optical information corresponding to the relevant glucose concentration could be presented by holography technology. The holographic diffraction is guided by Bragg's law (Fig. 11B), and the Bragg equation is  $\lambda_{\text{peak}} = 2 \times n \times d \times \sin \theta$ , where  $\lambda_{\text{peak}}$  is the wavelength of the scattered wave,  $d$  is the separation distance between two nanostructure-based layers,  $n$  is the average effective index, and  $\theta$  is the Bragg angle.<sup>113,114</sup> Generally, the holographic glucose-sensing film contains Bragg diffraction gratings produced by a single laser pulse wavelength. The Bragg diffraction gratings consist of a hydrogel-based substrate, light-sensitive materials, and glucose-sensitive agents that can reversibly bind with glucose molecules. Phenylboronic acid (PBA) derivatives are the most commonly used glucose-sensitive agents in holographic sensing since they have been identified as the best binding ligands with glucose in aqueous media.<sup>115</sup>

Fig. 11A illustrates the optical signal (light) generation process corresponding to the glucose concentration through a glucose-sensitive holographic film.<sup>113</sup> When the holographic film is illuminated by white light, the diffraction gratings will filter all colors except for the specific defined narrow band of color. Thus, the guided color could be controlled by changing  $d$ , which is a coefficient in the Bragg equation.<sup>116</sup> In this case,  $d$  is controlled by the environmental glucose concentration. If the glucose concentration increases, more glucose molecules will bind to PBA derivatives, which causes swelling of the flexible hydrogel, increasing  $d$ , and *vice versa*. The swelling or shrinking of the hydrogel-based sensor under different glucose concentrations results in the change of diffraction and further produces a visual color change.<sup>117</sup> Fig. 11B presents the schematic diagram for this process.<sup>114</sup> As the degree of hydrogel swelling deepens,  $d$  also increases, and a 'red shift' will be obtained in the diffracted light.

Holographic sensing technology is considered a promising biomedical optical sensing platform due to its high selectivity, stability, and low preparation cost. It has been applied to detect and quantify glucose concentration in both artificial and *in vitro* human biofluids. Early studies

conducted by the Kabilan group reported that holographic sensors containing boronic-acid derivatives presented the sensing ability for glucose molecules.<sup>115,118,119</sup> They also pointed out that around 20 mol% of 3-acrylamido-phenylboronic acid (3-APB), which can reversibly bind with glucose through its *cis*-diol functional groups, can offer the maximal sensitivity to aqueous glucose solutions. However, 3-APB has a severe problem: it could bind with other carbohydrates containing the structure of *cis*-diols in biofluids, such as fructose and lactate. It may lead to overestimated glucose readout.<sup>113</sup> Solutions were reported such as by introducing 2-acrylamido-phenylboronate and 3-acrylamido-propyl-trimethylammonium chloride (ATMA) in the 3-APB incorporated holographic film, the selectivity for glucose can be improved under lactate and fructose interferences, respectively.<sup>113</sup> Worsley *et al.* developed a holographic system which consisted of 3-APB and ATMA for a long-time continuous glucose monitoring in human blood plasma with a glucose range of 54–594 mg dl<sup>-1</sup> (3–33 mM).<sup>85</sup> The results showed that the produced holographic glucose sensor performed well in continuous monitoring of blood plasma from 7 subjects without data lag or hysteresis, and 100% measurements were in the zone A and B of CEG analysis. Another study focused on the development of holographic sensors for urine glucose analysis. Yetisen *et al.* created holographic sensors containing 10–20 mol% of 3-APB to sense glucose concentrations of urine and evaluated the degree of interference to the position of Bragg peaks by the presence of fructose and lactate.<sup>86</sup> The sensors firstly measured glucose concentrations of artificial urine solutions and then human samples. Fig. 11C presents the Bragg peak shifts (within 510–1100 nm) of the holographic sensor (with 20 mol% 3-APB) in artificial urine solutions under pH 7.40. In the measurements of human urine solutions, the holographic CGM sensor (with 10 mol% 3-APB) provided a better accuracy ( $R = 0.79$ ) in comparison with a commercial colorimetric dipstick ( $R^2 = 0.28$ ). Moreover, it was also stated that the pH values could significantly influence the Bragg peak shifts. The interferences of lactate and fructose in urine were not eliminated, which are 1.57% (0.27 mM) and 0.32 (23.8  $\mu$ M), respectively. For continuous glucose measurements (CGM), an optical glucose sensor uses 2.5-dimensional photonic concavities imprinted with PBA functionalization hydrogel film. The coupling of PBA with *cis*-diols of glucose results in hydrogel expansion by  $\sim$ 2% for glucose concentration of 1 mM and  $\sim$ 34% for 200 mM.<sup>120</sup>

Several research groups have contributed to ophthalmic glucose sensors fabricated by holographic technology to measure the glucose concentration in tears.<sup>113,121</sup> Some of them have developed 3-APB-based holographic contact lens sensors that need to be operated by NIR technology and conducted clinical trials on animals' eyes, for example, rabbits.<sup>113</sup> However, the same as the fluorescence-based ophthalmic glucose sensors, the development of holographic glucose-sensing contact lens sensors is limited by the uncertain correlation between glucose in tear fluids and blood.



Although holographic sensing is considered a promising technology for low-cost and high-precision measurement of glucose monitoring, commercial holographic-based glucose sensors have not yet been developed. One of the challenges is that in bio-fluid measurements, other glucose-similar molecules (such as fructose and lactate) may also bind to the glucose-sensitive chelating agent and interfere with the shifting of the Bragg peak, resulting in an overestimation of glucose concentration. This greatly increases the difficulty for the improvements of formulations of the hydrogel-based holographic film. Moreover, the elasticity of the hydrogel substrate (the polymer matrix) may reduce during usage, which causes a decrease of Bragg peak shift wavelength. In addition, the holographic glucose sensor is also affected by the solution environment, such as pH and temperature, which means that individual calibration is needed for the measurement on different subjects.

**3.2.8 Hydrogel glucose sensing.** Hydrogel materials can be functionalized and designed for reversible change by swelling and contracting when encountering external stimuli such as glucose, temperature, pH, humidity, and biomolecule binding.<sup>122–125</sup> Hydrogel functionalized with phenylboronic acid (PBA) is one of the common glucose-sensing techniques.<sup>126,127</sup> Many researchers have adopted this approach for glucose sensing applications, as also discussed in holographic sensors. A reasonable number of published reports in this area is evidence of promising hydrogel applications for achieving higher sensitivity and fast response.<sup>127</sup> Phenylboronic acid is considered glucose-responsive due to its affinity for diol-containing molecules. The PBA present in the hydrogel matrix interacts with the glucose, leading to the volumetric change in the hydrogel, which can be seen in Fig. 12A. A glucose-responsive hydrogel polyacrylamide–poly(ethylene glycol) (PEG) with boronic acid was reported in 2003.<sup>122</sup> These functional groups are prepositioned in the hydrogel photonic crystal to make a supramolecular complex, increasing hydrogel cross-linking. A blue shift in photonic crystal diffraction was observed over physiological glucose concentrations. In addition, it was found that these sensors were selective for glucose over fructose, galactose, and mannose. In 2009, Sven *et al.* reported another hydrogel-based optical fiber glucose sensor. The hydrogel was attached at the tip of the fiber as a Fabry–Perot cavity. Boronic acid was used as a glucose sensitive stimulus in acrylamide-based hydrogel.<sup>128</sup>

A report published in 2013 discussed the effect of PBA structural change upon interaction with glucose molecules. To fully understand these interactions, the hydrogel was functionalized with different classes of PBAs. This study includes different structural parameters like boronic acid position at the phenyl ring, different cross-linkers to the hydrogel backbone, and different classes of PBA. It was found that PBAs that cause a linear volumetric change in response to glucose show large hysteresis and slow response. On the other hand, PBAs with nonlinear volumetric change show minor hysteresis and rapid response.<sup>127</sup> Therefore, the

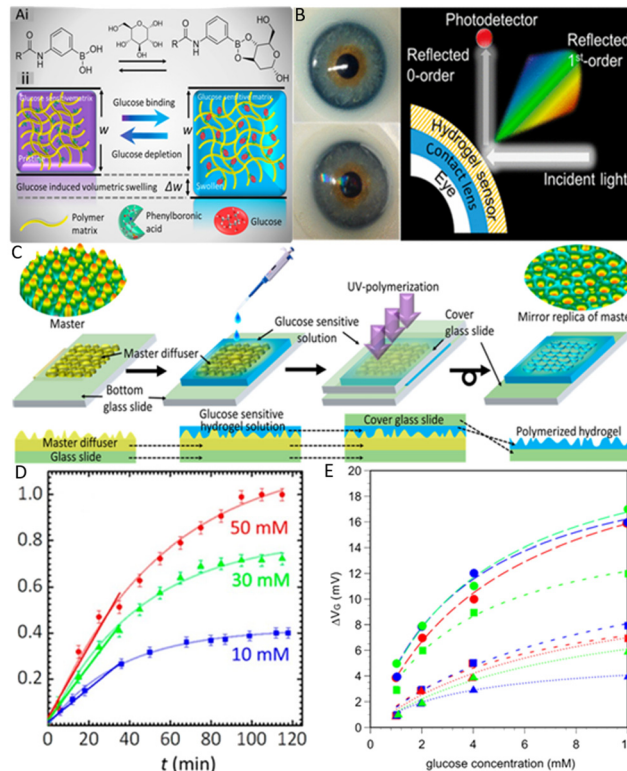


**Fig. 12** Hydrogel glucose sensing. (A) Schematic illustration of functionalized PBA hydrogel matrix swelling in glucose solution. (i) Molecular structure of the glucose-binding procedure that triggers swelling of the hydrogel matrix. (ii) Volumetric change illustration with glucose introduction into the glucose-sensitive hydrogel matrix.<sup>126</sup> Reproduced from ref. 126 with permission from ACS, Copyrights 2018. (B) Glucose sensor integrated contact lens. Starting from the left top with the commercial lens placed on an artificial eye. Under that the contact lens sensor is attached to the same eye model and on the right side the schematic diagram of contact lens measurement setup is represented.<sup>129</sup> Reproduced from ref. 129 with permission from ACS, Copyrights 2018. (C) Imprinting of a micro diffuser in hydrogel films. Schematic of the whole process starting from drop-casting of hydrogel-PBA solution on the master diffuser to the UV-polymerization process. In the end mirror replica of a micro diffuser is obtained on glucose-sensitive hydrogel.<sup>126</sup> Reproduced from ref. 126 with permission from ACS, Copyrights 2018. (D) Measurement of a hydrogel-PBA-based glucose sensor in transmission mode over the glucose concentrations of 10, 30 & 50 mM for a period of 120 min.<sup>126</sup> Reproduced from ref. 126 with permission from ACS, Copyrights 2018. (E) Glucose sensing using a hydrogel field-effect transistor (FET) in the glucose concentration range of 10  $\mu$ M to 40 mM. Each sample solution was measured with a FET hydrogel sensor. The blue line represents the phosphate-buffered saline solution without glucose, and the red line represents the signal recorded when the glucose solution was added to the phosphate-buffered saline solution.<sup>131</sup> Reproduced from ref. 131 with permission from Taylor & Francis, Copyrights 2017.

hydrogel optical fiber sensor was reported for continuous and real-time glucose sensing. The hydrogel fiber was fabricated with a poly(acrylamide-co-poly(ethylene glycol) diacrylate) core and functionalized with PBA.<sup>35</sup>

Functionalized hydrogel-based glucose sensors were acknowledged for wearable contact lenses. This sensor uses a photonic microstructure with a periodicity of 1.6  $\mu$ m. The



printing of these microstructures was applied in a functionalized PBA hydrogel-base. Upon swelling, the distance between the microstructure changes. A relationship was established between the periodicity and concentration of glucose from 0–50 mM. The sensor showed a sensitivity of 12 nm mM<sup>-1</sup>. A commercial contact lens was used to integrate this sensor for CGM (schematic of the sensor can be seen in Fig. 12B). The output signal was recorded using a smartphone camera. The fast response of 3 s and 4 min of saturation time were achieved in CGM mode.<sup>129</sup> In the same year, Mohammad reported a functionalized PBA hydrogel-based optical fiber sensor. A microstructure optical diffuser was imprinted on the phenylboronic hydrogel that can be seen in Fig. 12C. This diffuser structure on this film was established on the laser-inscribed array of microlenses. These lenses focus the light in different directions and points, which results in the diffused profile for transmission and reflections of light. The change in volume and intensity of transmitted light can be observed with increasing glucose concentration.<sup>126</sup> Another optical fiber sensor for CGM using the glucose-responsive (PBA) hydrogel matrix was reported in 2019. An asymmetric microlens array was imprinted on the hydrogel matrix and attracted to the multimode optical fiber tip during photo-polymerization. The glucose concentration was measured in the physiological range. The output signal was read by a smartphone and optical power meter. This setup showed a higher sensitivity of 2.6 μW mM<sup>-1</sup>. Glucose sensing in both transmission and reflection modes was measured in the physiological glucose range.<sup>130</sup>

A protective hydrogel coating was reported for implanted glucose sensors from biofouling. For this, 2,3-dihydroxy propyl methacrylate (DHPMA) and hydroxyethyl methacrylate (HEMA) were used along with ethylene glycol dimethacrylate (EGDMA) and *N*-vinyl-2-pyrrolidinone (VP) to improve the mechanical properties. The sensors were implanted in rats and tested once a week for 4 weeks. Improved linearity from 2–30 mM along with a fast response time of 5 min was recorded. In addition, the hydrogel coating implanted sensors kept functioning for 21 to 28 days.<sup>132</sup>

Sawayama and Takeuchi reported biocompatible fluorescence-base hydrogel sensors. Polyethylene glycol (PEG) hydrogel was fabricated using a glucose-responsive fluorescence dye (GF-PEG). This fluorescence dye is attached to the implanted device for CGM in diabetic rats and found to be stable for around 45 days. This device is also used for glucose monitoring in pigs with promising results. Usually, the problem with hydrogel sensors functionalized with PBA is that they degrade over time after implantation, and the fluorescence intensity will decrease. However, adding catalase and superoxide dismutase (antioxidant enzymes) into hydrogel sensors can overcome degradation.<sup>133</sup>

A radio frequency (RF) resonator based on hydrogel with PBA was reported by Dautta *et al.* for glucose monitoring. These sensors were scalable, stretchable, very tiny, and needed no power and microelectronics with ease in reading output remotely. The read-out was recorded in the form of a shift in

the RF signal. They showed a high sensitivity of ~10% shift to 50 MHz per 150 mg dL<sup>-1</sup> of glucose. On the other hand, a long lifetime of 45 days was observed for these sensors with no hysteresis or signal drop.<sup>134</sup> Hydrogel functionalized with vinyl-phenylboronic acid (VPBA) was used in a field-effect transistor for higher sensitivity of glucose. This device leads to higher sensitivity (Fig. 12E) in ionic charge detection, enabling specific glucose detection with biocompatibility.<sup>131</sup>

Hydrogel sensors are also reported in the literature for glucose-sensing in interstitial fluids like saliva, sweat, and tears.<sup>135–139</sup> Proteases, glucose transporters, have been found in the human eye cornea and are responsible for transporting glucose to tears. As a result, tears can be used to monitor the blood glucose level. For example, a hydrogel sensor comprising a 2D photonic crystal was reported for glucose sensing in tears.<sup>136</sup> The photonic crystal was based on a glucose-sensitive monolayered colloidal crystal (MCC) along with self-assembled polystyrene nanoparticles. Later this 2D crystal was coated with hydrogel (4-boronobenzaldehyde-functionalized poly(vinyl alcohol)). The color change was observed with the diffraction of visible light with changing glucose concentration (0 to 20 mM) with a fast response time of 180 s. Besides tears, sweat can also be used to monitor blood glucose because blood arteries around the sweat gland are well developed. For example, a hydrogel sensor was reported to detect glucose levels in sweat.<sup>137</sup> The sensor was composed of wearable hydrogel patches for electrochemical glucose sensing in natural sweat. The sensors were placed on the palm, fingers, and backside of the human hand, and the sweat glucose level was recorded in a rest position for 7 hours. The results obtained were found to be in good agreement with glucometer readings. Lastly, glucose sensing in saliva has also been reported. For example, a quartz crystal microbalance-based sensor coated with a hydrogel material was reported for glucose sensing in saliva.<sup>139</sup> The sensors showed the ultralow limit of detection of 3 mg L<sup>-1</sup> for glucose concentration in saliva. The hydrogel coating provides sufficient binding sites for glucose molecules for detection. Although the glucose concentration in saliva is deficient (1/50 to 1/100) compared to blood glucose, this proposed sensor provides a highly beneficial approach for detecting ultra-low glucose concentrations.

Besides high precision, fast response time, sensitivity, and biocompatibility, the functionalized hydrogel faces many challenges. As discussed above, it can be used in various ways, including implanted sensors, fluorescence sensing, RF resonators, and transistors and attaching them to optical fiber. The decrease in fluorescence intensity, the degradation of implanted sensors, the elasticity of the hydrogel matrix, and the presence of other similar glucose molecules are the biggest challenges that need to be addressed while working with hydrogel glucose sensors.

## 4. Discussion and forward-looking

The optical sensing technologies for CGM have been explored for several decades, while few optical-based glucose sensors





techniques to solve problems such as interference, attenuation, and noise of signals.<sup>16,17</sup> Therefore, more effective algorithms, statistical analysis techniques, and mathematical models to achieve the precise distinction of glucose molecules are suggested as the main directions for developing optical CGM sensors in the future.

## 5. Conclusion

In summary, major commercial CGM devices and optical glucose sensing technologies were introduced. Although electrochemical glucose sensors have taken a large amount of the glucose sensor market, developing the first fluorescence-based CGM (the Senseonics Eversense) brings a promising future for optical glucose sensing technologies. Advantages and limitations for each of the seven optical technologies were discussed. Among them, fluorescence sensing and holographic sensing are considered to have high potential in developing advanced non-invasive CGM systems. It is suggested that further research on optical CGM sensors should put effort into developing data processing methods, including algorithms, statistical analysis, and mathematical models, to achieve highly accurate measurements in glucose concentration monitoring.

## Conflicts of interest

There are no conflicts to declare.

## Acknowledgements

N. J. acknowledges the National Natural Science Foundation of China (No. 82102182) and the Fundamental Research Funds for the Central Universities (No. YJ202152). The authors acknowledge Khalifa University for KU-KAIST Joint Research Center (8474000220-KKJRC-2019-Health1) research funding in support on this research. The authors also acknowledge Sandoq Al Watan LLC and Aldar Properties for the research funding (SWARD Program – AWARD, 8434000391-EX2020-044).

## References

- 1 *Diabetes*, 2018, <https://www.who.int/news-room/fact-sheets/detail/diabetes>, (Accessed 04 February 2020).
- 2 P. Saeedi, I. Petersohn, P. Salpea, B. Malanda, S. Karuranga, N. Unwin, S. Colagiuri, L. Guariguata, A. A. Motala, K. Ogurtsova, J. E. Shaw, D. Bright and R. Williams, Global and regional diabetes prevalence estimates for 2019 and projections for 2030 and 2045: Results from the International Diabetes Federation Diabetes Atlas, 9th edition, *Diabetes Res. Clin. Pract.*, 2019, **157**, 107843.
- 3 *The top 10 causes of death*, 2018, <https://www.who.int/news-room/fact-sheets/detail/the-top-10-causes-of-death>, (Accessed 05 February 2020).
- 4 *IDF Diabetes Atlas|10th edn*, 2022. <https://diabetesatlas.org/>.
- 5 K. Gohil and D. Enhoffer, Diabetes market grows ever more crowded, *P T*, 2014, **39**(12), 877–879.
- 6 A. More, *Global diabetes drugs market 2020 to showing impressive*, 2020, <https://www.globenewswire.com/news-release/2020/03/02/1993439/0/en/Global-Diabetes-Drugs-Market-2020-to-Showing-Impressive-Growth-by-2025-Industry-Trends-Share-Size-Top-Key-Players-Analysis-and-Forecast-360-Market-Updates.html>.
- 7 S. Smyth and A. Heron, Diabetes and obesity: the twin epidemics, *Nat. Med.*, 2006, **12**(1), 75–80.
- 8 J. L. Rains and S. K. Jain, Oxidative stress, insulin signaling, and diabetes, *Free Radical Biol. Med.*, 2011, **50**(5), 567–575.
- 9 A. K. Foulis, The pathology of islets in diabetes, *Eye*, 1993, **7**(2), 197–201.
- 10 A. K. Foulis, Pancreatic pathology in type 1 diabetes, *J. Med. Virol.*, 2009, **81**(1), 195.
- 11 G. Klöppel, M. Löhr, K. Habich, M. Oberholzer and P. U. Heitz, Islet pathology and the pathogenesis of type 1 and type 2 diabetes mellitus revisited, *Surv. Synth. Pathol. Res.*, 1985, **4**(2), 110–125.
- 12 A. D. Deshpande, M. Harris-Hayes and M. Schootman, Epidemiology of diabetes and diabetes-related complications, *Phys. Ther.*, 2008, **88**(11), 1254–1264.
- 13 J. Bidonde, B. C. Fagerlund, K. B. Frønsdal, U. H. Lund and B. Robberstad, *FreeStyle Libre Flash glucose self-monitoring system: A single-technology assessment*, Knowledge Centre for the Health Services at The Norwegian Institute of Public Health (NIPH), 2017, pp. 1–7.
- 14 P. B. Sandesara, W. T. O'Neal, H. M. Kelli, A. Samman-Tahhan, M. Hammadah, A. A. Quyyumi and L. S. Sperling, The prognostic significance of diabetes and microvascular complications in patients with heart failure with preserved ejection fraction, *Diabetes Care*, 2018, **41**(1), 150–155.
- 15 L. J. Diann, W. Hsiang-Lin, L. Jer-Chuan, W. C. Zu, K. Shi-Wen, H. C. Hsun, L. Wei-Chen, L. Chien-Hsing, K. Mei-Teng and P. Dee, Impaired glucose tolerance and impaired fasting glucose share similar underlying pathophysiologies, *Tohoku J. Exp. Med.*, 2007, **212**(4), 349–357.
- 16 W. V. Gonzales, A. T. Mobashsher and A. Abbosh, The progress of glucose monitoring: A review of invasive to minimally and non-invasive techniques, devices and sensors, *Sensors*, 2019, **19**(4), 800.
- 17 I. L. Jernelv, K. Milenko, S. S. Fuglerud, D. R. Hjelme, R. Ellingsen and A. Aksnes, A review of optical methods for continuous glucose monitoring, *Appl. Spectrosc. Rev.*, 2019, **54**(7), 543–572.
- 18 C.-F. So, K.-S. Choi, T. K. Wong and J. W. Chung, Recent advances in noninvasive glucose monitoring, *Med. Devices*, 2012, **5**(1), 45–52.
- 19 E. Cauza, U. Hanusch-Enserer, B. Strasser, B. Ludvik, K. Kostner, A. Dunky and P. Haber, Continuous glucose monitoring in diabetic long distance runners, *Int. J. Sports Med.*, 2005, **26**, 774–780.
- 20 B. Bonora, A. Maran, S. Ciciliot, A. Avogaro and G. P. Fadini, Head-to-head comparison between flash and continuous glucose monitoring systems in outpatients with type 1 diabetes, *J. Endocrinol. Invest.*, 2016, **39**(12), 1391–1399.



- 21 M. A. Pleitez, T. Lieblein, A. Bauer, O. Hertzberg, H. von Lilienfeld-Toal and W. Mantele, In vivo noninvasive monitoring of glucose concentration in human epidermis by mid-infrared pulsed photoacoustic spectroscopy, *Anal. Chem.*, 2013, **85**(2), 1013–1020.
- 22 F. Guido, L. Manuela, P. Stefan, W. Antje, K. Ulrik and H. Cprnelia, Measurement performance of two continuous tissue glucose monitoring systems intended for replacement of blood glucose monitoring, *Diabetes Technol. Ther.*, 2018, **20**(8), 541–549.
- 23 M. S. Steiner, A. Duerkop and O. S. Wolfbeis, Optical methods for sensing glucose, *Chem. Soc. Rev.*, 2011, **40**(9), 4805–4839.
- 24 M. Mortellaro and A. DeHennis, Performance characterization of an abiotic and fluorescent-based continuous glucose monitoring system in patients with type 1 diabetes, *Biosens. Bioelectron.*, 2014, **61**, 227–231.
- 25 X. Sun and T. D. James, Glucose sensing in supramolecular chemistry, *Chem. Rev.*, 2015, **115**(15), 8001–8037.
- 26 L. Heinemann and D. Boecker, Lancing: quo vadis?, *J. Diabetes Sci. Technol.*, 2011, **5**(4), 966–981.
- 27 J. Zhang, W. Hodge, C. Hutnick and X. Wang, Noninvasive diagnostic devices for diabetes through measuring tear glucose, *J. Diabetes Sci. Technol.*, 2011, **5**(1), 166–172.
- 28 L. C. Clark Jr. and C. Lyons, Electrode systems for continuous monitoring in cardiovascular surgery, *Ann. N. Y. Acad. Sci.*, 1962, **102**(1), 29–45.
- 29 J. Wang, Electrochemical glucose biosensors, *Chem. Rev.*, 2008, **108**(2), 814–825.
- 30 J. Pettus and S. V. Edelman, Recommendations for using real-time continuous glucose monitoring (rtCGM) data for insulin adjustments in type 1 diabetes, *J. Diabetes Sci. Technol.*, 2017, **11**(1), 138–147.
- 31 S. P. Nichols, A. Koh, W. L. Storm, J. H. Shin and M. H. Schoenfisch, Biocompatible materials for continuous glucose monitoring devices, *Chem. Rev.*, 2013, **113**(4), 2528–2549.
- 32 L. Bally, H. Thabit, S. Hartnell, E. Anderegg, Y. Ruan, M. E. Wilinska, M. L. Evans, M. M. Wertli, A. P. Coll, C. Stettler and R. Hovorka, Closed-loop insulin delivery for glycemic control in noncritical care, *N. Engl. J. Med.*, 2018, **379**(6), 547–556.
- 33 H.-C. Yeh, T. T. Brown, N. Maruthur, P. Ranasinghe, Z. Berger, Y. D. Suh, L. M. Wilson, E. B. Haberl, J. Brick, E. B. Bass and S. H. Golden, Comparative effectiveness and safety of methods of insulin delivery and glucose monitoring for diabetes mellitus, *Ann. Intern. Med.*, 2012, **157**(5), 336.
- 34 G. Aleppo, L. M. Laffel, A. J. Ahmann, I. B. Hirsch, D. F. Kruger, A. Peters, R. S. Weinstock and D. R. Harris, A practical approach to using trend arrows on the Dexcom G5 CGM system for the management of adults with diabetes, *J. Endocr. Soc.*, 2017, **1**(12), 1445–1460.
- 35 A. K. Yetisen, N. Jiang, A. Fallahi, Y. Montelongo, G. U. Ruiz-Esparza, A. Tamayol, Y. S. Zhang, I. Mahmood, S.-A. Yang, K. S. Kim, H. Butt, A. Khademhosseini and S.-H. Yun, Glucose-sensitive hydrogel optical fibers functionalized with phenylboronic acid, *Adv. Mater.*, 2017, **29**(15), 1606380.
- 36 D. B. Keenan, J. J. Mastrototaro, G. Voskanyan and G. M. Steil, Delays in minimally invasive continuous glucose monitoring devices: A review of current technology, *J. Diabetes Sci. Technol.*, 2009, **3**(5), 1207–1214.
- 37 T. M. Gross, B. W. Bode, D. Einhorn, D. M. Kayne, J. H. Reed, N. H. White and J. J. Mastrototaro, Performance evaluation of the MiniMed® continuous glucose monitoring system during patient home use, *Diabetes Technol. Ther.*, 2000, **2**(1), 49–56.
- 38 J. Mastrototaro, The MiniMed continuous glucose monitoring system, *J. Pediatr. Endocrinol. Metab.*, 1999, **12**(3), 751–758.
- 39 S. Newman, D. Cooke, A. Casbard, S. Walker, S. Meredith, A. Nunn, L. Steed, A. Manca, M. Sculpher, M. Barnard, D. Kerr, J. Weaver, J. Ahlquist and S. Hurel, A randomised controlled trial to compare minimally invasive glucose monitoring devices with conventional monitoring in the management of insulin-treated diabetes mellitus (MITRE), *Health Technol. Assess.*, 2009, **13**(28), 1–194.
- 40 Y. J. Heo and S.-H. Kim, Toward long-term implantable glucose biosensors for clinical use, *Appl. Sci.*, 2019, **9**(10), 2158.
- 41 L. Overend, E. Simpson and T. Grimwood, Qualitative analysis of patient responses to the ABCD FreeStyle Libre audit questionnaire, *Practical Diabetes*, 2019, **36**(2), 45–50.
- 42 E. Oppel, S. Kamann, F. X. Reichl and C. Hogg, The Dexcom glucose monitoring system—An isobornyl acrylate-free alternative for diabetic patients, *Contact Dermatitis*, 2019, **81**(1), 32–36.
- 43 B. D. Wang, W. Qiao, W. W. Ye, X. L. Wang, Y. Q. Liu, Y. X. Wang and Y. F. Xiao, Comparison of continuous glucose monitoring between Dexcom G4 platinum and HD-XG systems in nonhuman primates (Macaca Fascicularis), *Sci. Rep.*, 2017, **7**(1), 9596.
- 44 J. Smith, *The pursuit of noninvasive glucose: Hunting the deceitful Turkey*, 2006.
- 45 I. M. E. Wentholt, J. B. L. Hoekstra, A. Zwart and J. H. Devries, Pendra goes Dutch: lessons for the CE mark in Europe, *Diabetologia*, 2005, **48**(6), 1055–1058.
- 46 S. A. Weinzimer, Analysis: PENDRA: The once and future noninvasive continuous glucose monitoring device?, *Diabetes Technol. Ther.*, 2004, **6**(4), 442–444.
- 47 H. Lenzen, B. A. Barrow, S. White and R. R. Holman, A non-invasive frequent home blood glucose monitor, *Practical Diabetes Int.*, 2002, **19**(4), 101–103.
- 48 G. Campetelli, D. Zumoffen and M. Basualdo, Improvements on noninvasive blood glucose biosensors using wavelets for quick fault detection, *J. Sens.*, 2011, **2011**, 368015.
- 49 V. D. Funtanilla, P. Candidate, T. Caliendo and O. Hilas, Continuous glucose monitoring: A review of available systems, *P T*, 2019, **44**(9), 550.
- 50 D. Rathod, C. Dickinson, D. Egan and E. Dempsey, Platinum nanoparticle decoration of carbon materials with



- applications in non-enzymatic glucose sensing, *Sens. Actuators, B*, 2010, **143**(2), 547–554.
- 51 S. Park, H. Boo and T. D. Chung, Electrochemical non-enzymatic glucose sensors, *Anal. Chim. Acta*, 2006, **556**(1), 46–57.
  - 52 Y. Bai, Y. Sun and C. Sun, Pt–Pb nanowire array electrode for enzyme-free glucose detection, *Biosens. Bioelectron.*, 2008, **24**(4), 579–585.
  - 53 D. Arif, Z. Hussain, M. Sohail, M. A. Liaqat, M. A. Khan and T. Noor, A non-enzymatic electrochemical sensor for glucose detection based on Ag@TiO<sub>2</sub>@Metal-Organic framework (ZIF-67) nanocomposite, *Front. Chem.*, 2020, **24**(4), 579–585.
  - 54 Y. M. Chitare, S. B. Jadhav, P. N. Pawaskar, V. V. Magdum, J. L. Gunjekar and C. D. Lokhande, Metal oxide-based composites in nonenzymatic electrochemical glucose sensors, *Ind. Eng. Chem. Res.*, 2021, **60**(50), 18195–18217.
  - 55 G. Wang, X. He, L. Wang, A. Gu, Y. Huang, B. Fang, B. Geng and X. Zhang, Non-enzymatic electrochemical sensing of glucose, *Microchim. Acta*, 2013, **180**(3–4), 161–186.
  - 56 X. Niu, X. Li, J. Pan, Y. He, F. Qiu and Y. Yan, Recent advances in non-enzymatic electrochemical glucose sensors based on non-precious transition metal materials: opportunities and challenges, *RSC Adv.*, 2016, **6**(88), 84893–84905.
  - 57 I. Taurino, G. Sanz , F. Mazzei, G. Favero, G. De Micheli and S. Carrara, Fast synthesis of platinum nanopetals and nanospheres for highly-sensitive non-enzymatic detection of glucose and selective sensing of ions, *Sci. Rep.*, 2015, **5**(1), 15277.
  - 58 T. Unm ssig, A. Weltin, S. Urban, P. Daubinger, G. A. Urban and J. Kieninger, Non-enzymatic glucose sensing based on hierarchical platinum micro-/nanostructures, *J. Electroanal. Chem.*, 2018, **816**(1), 215–222.
  - 59 W. McCormick, P. McDonagh, J. Doran and D. McCrudden, Covalent immobilisation of a nanoporous platinum film onto a gold screen-printed electrode for highly stable and selective non-enzymatic glucose sensing, *Catalysts*, 2021, **11**(10), 1161.
  - 60 J. C. Claussen, S. S. Kim, A. Haque, M. S. Artilles, D. M. Porterfield and T. S. Fisher, Electrochemical glucose biosensor of platinum nanospheres connected by carbon nanotubes, *J. Diabetes Sci. Technol.*, 2010, **4**(2), 312–319.
  - 61 E. R. Mamleyev, P. G. Weidler, A. Nefedov, D. V. Szab , M. Islam, D. Mager and J. G. Korvink, Nano- and microstructured copper/copper oxide composites on laser-induced carbon for enzyme-free glucose sensors, *ACS Appl. Nano Mater.*, 2021, **4**(12), 13747–13760.
  - 62 Y. Ding, Y. Liu, J. Parisi, L. Zhang and L. Yu, A novel NiO–Au hybrid nanobelts based sensor for sensitive and selective glucose detection, *Biosens. Bioelectron.*, 2011, **28**(1), 393–398.
  - 63 G. Purvinis, B. D. Cameron and D. M. Altrogge, Noninvasive polarimetric-based glucose monitoring: an in vivo study, *J. Diabetes Sci. Technol.*, 2011, **5**(2), 380–387.
  - 64 M. A. Pleitez, O. Hertzberg, A. Bauer, M. Seeger, T. Lieblein, H. V. Lilienfeld-Toal and W. M ntele, Photothermal deflectometry enhanced by total internal reflection enables non-invasive glucose monitoring in human epidermis, *Analyst*, 2015, **140**(2), 483–488.
  - 65 O. Hertzberg, A. Bauer, A. K uderle, M. A. Pleitez and W. M ntele, Depth-selective photothermal IR spectroscopy of skin: potential application for non-invasive glucose measurement, *Analyst*, 2017, **142**(3), 495–502.
  - 66 M. Goodarzi and W. Saeys, Selection of the most informative near infrared spectroscopy wavebands for continuous glucose monitoring in human serum, *Talanta*, 2016, **146**, 155–165.
  - 67 E. Ryckeboer, R. Bockstaele, M. Vanslembrouck and R. Baets, Glucose sensing by waveguide-based absorption spectroscopy on a silicon chip, *Biomed. Opt. Express*, 2014, **5**(5), 1636–1648.
  - 68 J. T. Olesberg, L. Liu, V. V. Zee and M. A. Arnold, In vivo near-infrared spectroscopy of rat skin tissue with varying blood glucose levels, *Anal. Chem.*, 2006, **78**(1), 215–223.
  - 69 K. Maruo, T. Oota, M. Tsurugi, T. Nakagawa, H. Arimoto, M. Hayakawa, M. Tamura, Y. Ozaki and Y. Yamada, Noninvasive near-infrared blood glucose monitoring using a calibration model built by a numerical simulation method: Trial application to patients in an intensive care unit, *Appl. Spectrosc.*, 2006, **60**(12), 1423–1431.
  - 70 L. Ben Mohammadi, T. Klotzbuecher, S. Sigloch, K. Welzel, M. Goeddel, T. R. Pieber and L. Schaupp, Clinical performance of a low cost near infrared sensor for continuous glucose monitoring applied with subcutaneous microdialysis, *Biomed. Microdevices*, 2015, **17**(4), 73.
  - 71 H. M. Heise, R. Marbach, T. Koschinsky and F. A. Gries, Multicomponent assay for blood substrates in human plasma by mid-infrared spectroscopy and its evaluation for clinical analysis, *Appl. Spectrosc.*, 1994, **48**(1), 85–95.
  - 72 M. Brandstetter, L. Volgger, A. Genner, C. Jungbauer and B. Lendl, Direct determination of glucose, lactate and triglycerides in blood serum by a tunable quantum cascade laser-based mid-IR sensor, *Appl. Phys. B: Lasers Opt.*, 2013, **110**(2), 233–239.
  - 73 S. Liakat, K. A. Bors, L. Xu, C. M. Woods, J. Doyle and C. F. Gmachl, Noninvasive in vivo glucose sensing on human subjects using mid-infrared light, *Biomed. Opt. Express*, 2014, **5**(7), 2397–2404.
  - 74 C. Vrancic, N. Kroger, N. Gretz, S. Neudecker, A. Pucci and W. Petrich, A quantitative look inside the body: Minimally invasive infrared analysis in vivo, *Anal. Chem.*, 2014, **86**(21), 10511–10514.
  - 75 S. Kino, S. Omori, T. Katagiri and Y. Matsuura, Hollow optical-fiber based infrared spectroscopy for measurement of blood glucose level by using multi-reflection prism, *Biomed. Opt. Express*, 2016, **7**(2), 701–708.
  - 76 C. C. Pelletier, J. L. Lambert and M. Borchert, Determination of glucose in human aqueous humor using Raman spectroscopy and designed-solution calibration, *Appl. Spectrosc.*, 2005, **59**(8), 1024–1031.



- 77 C. R. Kong, I. Barman, N. C. Dingari, J. W. Kang, L. Galindo, R. R. Dasari and M. S. Feld, A novel non-imaging optics based Raman spectroscopy device for transdermal blood analyte measurement, *AIP Adv.*, 2011, **1**(3), 32175.
- 78 W. C. Shih, K. L. Bechtel and M. V. Rebec, Noninvasive glucose sensing by transcutaneous Raman spectroscopy, *J. Biomed. Opt.*, 2015, **20**(5), 051036.
- 79 K. Ma, J. M. Yuen, N. C. Shah, J. T. Walsh, M. R. Glucksberg and R. P. Van Duyne, In vivo, transcutaneous glucose sensing using surface-enhanced spatially offset raman spectroscopy: Multiple rats, improved hypoglycemic accuracy, low incident power, and continuous monitoring for greater than 17 days, *Anal. Chem.*, 2011, **83**(23), 9146–9152.
- 80 J. Kottmann, J. M. Rey and M. W. Sigrist, Mid-infrared photoacoustic detection of glucose in human skin: towards non-invasive diagnostics, *Sensors*, 2016, **16**(10), 1663.
- 81 R. Dutt-Ballerstadt, C. Evans, A. P. Pillai, E. Orzeck, R. Drabek, A. Gowda and R. McNichols, A human pilot study of the fluorescence affinity sensor for continuous glucose monitoring in diabetes, *J. Diabetes Sci. Technol.*, 2012, **6**(2), 362–370.
- 82 A. J. Müller, M. Knuth, K. S. Nikolaus, R. Krivánek, F. Küster and C. Hasslacher, First clinical evaluation of a new percutaneous optical fiber glucose sensor for continuous glucose monitoring in diabetes, *J. Diabetes Sci. Technol.*, 2013, **7**(1), 13–23.
- 83 K. Larin, M. Motamedi, T. Ashitkov and R. Esenaliev, Specificity of noninvasive blood glucose sensing using optical coherence tomography technique: A pilot study, *Phys. Med. Biol.*, 2003, **48**, 1371–1390.
- 84 R. A. Gabbay and S. Sivarajah, Optical coherence tomography-based continuous noninvasive glucose monitoring in patients with diabetes, *Diabetes Technol. Ther.*, 2008, **10**(3), 188–193.
- 85 G. J. Worsley, G. A. Tourniaire, K. E. S. Medlock, F. K. Sartain, H. E. Harmer, M. Thatcher, A. M. Horgan and J. Pritchard, Continuous blood glucose monitoring with a thin-film optical sensor, *Clin. Chem.*, 2007, **53**(10), 1820–1826.
- 86 A. K. Yetisen, Y. Montelongo, F. da Cruz Vasconcellos, J. L. Martinez-Hurtado, S. Neupane, H. Butt, M. M. Qasim, J. Blyth, K. Burling, J. B. Carmody, M. Evans, T. D. Wilkinson, L. T. Kubota, M. J. Monteiro and C. R. Lowe, Reusable, robust, and accurate laser-generated photonic nanosensor, *Nano Lett.*, 2014, **14**(6), 3587–3593.
- 87 J. Chen, M. A. Arnold and G. W. Small, Comparison of combination and first overtone spectral regions for near-infrared calibration models for glucose and other biomolecules in aqueous solutions, *Anal. Chem.*, 2004, **76**(18), 5405–5413.
- 88 P. S. Jensen and J. Bak, Near-infrared transmission spectroscopy of aqueous solutions: Influence of optical path length on signal-to-noise ratio, *Appl. Spectrosc.*, 2002, **56**(12), 1600–1606.
- 89 H. M. Heise, R. Marbach, T. Koschinsky and F. A. Gries, Noninvasive blood glucose sensors based on near-infrared spectroscopy, *Artif. Organs*, 1994, **18**(6), 439–447.
- 90 M. A. Arnold and G. W. Small, Noninvasive glucose sensing, *Anal. Chem.*, 2005, **77**(17), 5429–5439.
- 91 J. Liu, R. Liu and K. Xu, Accuracy of noninvasive glucose sensing based on near-infrared spectroscopy, *Appl. Spectrosc.*, 2015, **69**(11), 1313–1318.
- 92 Z. Yu, N. Jiang, S. G. Kazarian, S. Tasoglu and A. K. Yetisen, Optical sensors for continuous glucose monitoring - IOPscience, *Prog. Biomed. Eng.*, 2021, **3**(2), 22004.
- 93 S. Sharma, M. Goodarzi, J. Delanghe, H. Ramon and W. Saeys, Using experimental data designs and multivariate modeling to assess the effect of glycated serum protein concentration on glucose prediction from near-infrared spectra of human serum, *Appl. Spectrosc.*, 2014, **68**(4), 398–405.
- 94 A. K. Amerov, J. Chen, G. W. Small and M. A. Arnold, Scattering and absorption effects in the determination of glucose in whole blood by near-infrared spectroscopy, *Anal. Chem.*, 2005, **77**(14), 4587–4594.
- 95 K. Maruo and Y. Yamada, Near-infrared noninvasive blood glucose prediction without using multivariate analyses: introduction of imaginary spectra due to scattering change in the skin, *J. Biomed. Opt.*, 2015, **20**(4), 47003.
- 96 H. M. Heise, L. Küpper and L. N. Butvina, Attenuated total reflection mid-infrared spectroscopy for clinical chemistry applications using silver halide fibers, *Sens. Actuators, B*, 1998, **51**(1), 84–91.
- 97 E. Wiercigroch, E. Szafraniec, K. Czamara, M. Z. Pacia, K. Majzner, K. Kochan, A. Kaczor, M. Baranska and K. Malek, Raman and infrared spectroscopy of carbohydrates: A review, *Spectrochim. Acta, Part A*, 2017, **185**, 317–335.
- 98 G. S. Bumbrah and R. M. Sharma, Raman spectroscopy – Basic principle, instrumentation and selected applications for the characterization of drugs of abuse, *Egypt. J. Forensic Sci.*, 2016, **6**(3), 209–215.
- 99 N. Spegazzini, I. Barman, N. C. Dingari, R. Pandey, J. S. Soares, Y. Ozaki and R. R. Dasari, Spectroscopic approach for dynamic bioanalyte tracking with minimal concentration information, *Sci. Rep.*, 2015, **4**(1), 7013.
- 100 N. S. Oliver, C. Toumazou, A. E. G. Cass and D. G. Johnston, Glucose sensors: a review of current and emerging technology, *Diabetic Med.*, 2009, **26**(3), 197–210.
- 101 H.-C. Wang and A.-R. Lee, Recent developments in blood glucose sensors, *J. Food Drug Anal.*, 2015, **23**(2), 191–200.
- 102 *In vivo glucose sensing, Analytical and bioanalytical chemistry*, ed. P. Herman, D. D. Cunningham and J. A. Stenken, 2010, vol. 397(8), pp. 3159–3160.
- 103 P. W. Barone and M. S. Strano, Single walled carbon nanotubes as reporters for the optical detection of glucose, *J. Diabetes Sci. Technol.*, 2009, **3**(2), 242–252.
- 104 P. W. Barone, R. S. Parker and M. S. Strano, In vivo fluorescence detection of glucose using a single-walled carbon nanotube optical sensor: Design, fluorophore



- properties, advantages, and disadvantages, *Anal. Chem.*, 2005, **77**(23), 7556–7562.
- 105 L. Chen, E. Hwang and J. Zhang, Fluorescent nanobiosensors for sensing glucose, *Sensors*, 2018, **18**(5), 1440.
- 106 A. A. Essawy and M. S. Attia, Novel application of pyronin Y fluorophore as high sensitive optical sensor of glucose in human serum, *Talanta*, 2013, **107**, 18–24.
- 107 E. Scavetta, B. Ballarin and D. Tonelli, A cheap amperometric and optical sensor for glucose determination, *Electroanalysis*, 2010, **22**(4), 427–432.
- 108 R. Badugu, J. R. Lakowicz and C. D. Geddes, A glucose-sensing contact lens: from bench top to patient, *Curr. Opin. Biotechnol.*, 2005, **16**(1), 100–107.
- 109 H. Yao, A. J. Shum, M. Cowan, I. Lähdesmäki and B. A. Parviz, A contact lens with embedded sensor for monitoring tear glucose level, *Biosens. Bioelectron.*, 2011, **26**(7), 3290–3296.
- 110 J. S. Schultz, S. Mansouri and I. J. Goldstein, Affinity sensor: A new technique for developing implantable sensors for glucose and other metabolites, *Diabetes Care*, 1982, **5**(3), 245.
- 111 A. Fercher, W. Drexler, C. Hitzenberger and T. Lasser, Optical coherence tomography—principles and applications, *Rep. Prog. Phys.*, 2003, **66**(2), 239.
- 112 F. Adolf Friedrich, Optical coherence tomography – development, principles, applications, *Z. Med. Phys.*, 2010, **20**(4), 251–276.
- 113 A. K. Yetisen, I. Naydenova, F. Da Cruz Vasconcellos, J. Blyth and C. R. Lowe, Holographic sensors: three-dimensional analyte-sensitive nanostructures and their applications, *Chem. Rev.*, 2014, **114**(20), 10654.
- 114 N. Jiang, H. Butt, Y. Montelongo, F. Liu, S. Afewerki, G. L. Ying, Q. Dai, S. H. Yun and A. K. Yetisen, Laser interference lithography for the nanofabrication of stimuli-responsive bragg stacks, *Adv. Funct. Mater.*, 2018, **28**(24), 1702715.
- 115 S. Kabilan, J. Blyth, M. C. Lee, A. J. Marshall, A. Hussain, X.-P. Yang and C. R. Lowe, Glucose-sensitive holographic sensors, *J. Mol. Recognit.*, 2004, **17**(3), 162–166.
- 116 A. K. Yetisen, H. Qu, A. Manbachi, H. Butt, M. R. Dokmeci, J. P. Hinstroza, M. Skorobogatiy, A. Khademhosseini and S. H. Yun, Nanotechnology in textiles, *ACS Nano*, 2016, **10**(3), 3042.
- 117 A. J. Marshall, J. Blyth, C. A. B. Davidson and C. R. Lowe, pH-Sensitive holographic sensors, *Anal. Chem.*, 2003, **75**(17), 4423–4431.
- 118 S. Kabilan, A. J. Marshall, F. K. Sartain, M.-C. Lee, A. Hussain, X. Yang, J. Blyth, N. Karangu, K. James, J. Zeng, D. Smith, A. Domschke and C. R. Lowe, Holographic glucose sensors, *Biosens. Bioelectron.*, 2005, **20**(8), 1602–1610.
- 119 A. K. Yetisen, H. Butt, L. R. Volpatti, I. Pavlichenko, M. Humar, S. J. J. Kwok, H. Koo, K. S. Kim, I. Naydenova, A. Khademhosseini, S. K. Hahn and S. H. Yun, Photonic hydrogel sensors, *Biotechnol. Adv.*, 2016, **34**(3), 250–271.
- 120 M. Bajgrowicz-Cieslak, Y. Alqurashi, M. I. Elshereif, A. K. Yetisen, M. U. Hassan and H. Butt, Optical glucose sensors based on hexagonally-packed 2.5-dimensional photonic concavities imprinted in phenylboronic acid functionalized hydrogel films, *RSC Adv.*, 2017, **7**(85), 53916–53924.
- 121 A. Domschke, W. F. March, S. Kabilan and C. Lowe, Initial clinical testing of a holographic non-invasive contact lens glucose sensor, *Diabetes Technol. Ther.*, 2006, **8**(1), 89–93.
- 122 V. L. Alexeev, A. C. Sharma, A. V. Goponenko, S. Das, I. K. Lednev, C. S. Wilcox, D. N. Finegold and S. A. Asher, High ionic strength glucose-sensing photonic crystal, *Anal. Chem.*, 2003, **75**(10), 2316–2323.
- 123 I. Cobo, M. Li, B. S. Sumerlin and S. Perrier, Smart hybrid materials by conjugation of responsive polymers to biomacromolecules, *Nat. Mater.*, 2015, **14**(2), 143–159.
- 124 V. L. Alexeev, S. Das, D. N. Finegold and S. A. Asher, Photonic crystal glucose-sensing material for noninvasive monitoring of glucose in tear fluid, *Clin. Chem.*, 2004, **50**(12), 2353–2360.
- 125 A. K. Yetisen, H. Butt, F. D. C. Vasconcellos, Y. Montelongo, C. A. B. Davidson, J. Blyth, L. Chan, J. B. Carmody, S. Vignolini, U. Steiner, J. J. Baumberg, T. D. Wilkinson and C. R. Lowe, Light-directed writing of chemically tunable narrow-band holographic sensors, *Advanced, Opt. Mater.*, 2021, **2**(3), 250–254.
- 126 M. Elsharif, M. U. Hassan, A. K. Yetisen and H. Butt, Glucose sensing with phenylboronic acid functionalized hydrogel-based optical diffusers, *ACS Nano*, 2018, **12**(3), 2283–2291.
- 127 C. J. Zhang, M. D. Losego and P. V. Braun, Hydrogel-based glucose sensors: Effects of phenylboronic acid chemical structure on response, *Chem. Mater.*, 2013, **25**(15), 3239–3250.
- 128 S. Tierney, S. Volden and B. T. Stokke, Glucose sensors based on a responsive gel incorporated as a Fabry-Perot cavity on a fiber-optic readout platform, *Biosens. Bioelectron.*, 2009, **24**(7), 2034–2039.
- 129 M. Elsharif, M. U. Hassan, A. K. Yetisen and H. Butt, Wearable contact lens biosensors for continuous glucose monitoring using smartphones, *ACS Nano*, 2018, **12**(6), 5452–5462.
- 130 M. Elsharif, M. U. Hassan, A. K. Yetisen and H. Butt, Hydrogel optical fibers for continuous glucose monitoring, *Biosens. Bioelectron.*, 2019, **137**, 25–32.
- 131 T. Kajisa and T. Sakata, Glucose-responsive hydrogel electrode for biocompatible glucose transistor, *Sci. Technol. Adv. Mater.*, 2017, **18**(1), 26–33.
- 132 B. Z. Yu, C. Y. Wang, Y. M. Ju, L. West, J. Harmon, Y. Moussy and F. Moussy, Use of hydrogel coating to improve the performance of implanted glucose sensors, *Biosens. Bioelectron.*, 2008, **23**(8), 1278–1284.
- 133 J. Sawayama, T. Okitsu, A. Nakamata, Y. Kawahara and S. Takeuchi, Hydrogel glucose sensor with in vivo stable fluorescence intensity relying on antioxidant enzymes for continuous glucose monitoring, *iScience*, 2021, **23**(6), 101243.
- 134 M. Dautta, M. Alshetaiwi, J. Escobar and P. Tseng, Passive and wireless, implantable glucose sensing with phenylboronic acid hydrogel-interlayer RF resonators, *Biosens. Bioelectron.*, 2020, **151**, 112004.



- 135 R. Badugu, E. A. Reece and J. R. Lakowicz, Glucose-sensitive silicone hydrogel contact lens toward tear glucose monitoring, *J. Biomed. Opt.*, 2018, **23**(05), 1–9.
- 136 C. Chen, Z.-Q. Dong, J.-H. Shen, H.-W. Chen, Y.-H. Zhu and Z.-G. Zhu, 2D photonic crystal hydrogel sensor for tear glucose monitoring, *ACS Omega*, 2018, **3**(3), 3211–3217.
- 137 P.-H. Lin, S.-C. Sheu, C.-W. Chen, S.-C. Huang and B.-R. Li, Wearable hydrogel patch with noninvasive, electrochemical glucose sensor for natural sweat detection, *Talanta*, 2022, **241**, 123187.
- 138 K. Nagamine, T. Mano, A. Nomura, Y. Ichimura, R. Izawa, H. Furusawa, H. Matsui, D. Kumaki and S. Tokito, Noninvasive sweat-lactate biosensor employing a hydrogel-based touch pad, *Sci. Rep.*, 2019, **9**(1), 10102.
- 139 Q. Dou, Z. Zhang, Y. Wang, S. Wang, D. Hu, Z. Zhao, H. Liu and Q. Dai, Ultrasensitive poly(boric acid) hydrogel-coated quartz crystal microbalance sensor by using UV pressing-assisted polymerization for saliva glucose monitoring, *ACS Appl. Mater. Interfaces*, 2020, **12**(30), 34190–34197.

